LAMELIS
Lasers in Medicine and Life Sciences

TOTAL INTERNAL REFLECTION FLUORESCENCE MICROSCOPY

principles & applications

Beáta Bugyi

UNIVERSITY OF PÉCS – MEDICAL SCHOOL – DEPARTMENT OF BIOPHYSICS
CYTOSKELETAL DYNAMICS LAB
http://cytoskeletaldynamics.wix.com/mysite

OVERVIEW

CLASSICAL RESOLUTION LIMIT OF THE LIGHT MICROSCOPE

TOTAL INTERNAL REFLECTION FLUORESCENCE MICROSCOPY

- HISTORICAL PERSPECTIVES
- PHYSICAL PRINCIPLES
- TECHNICAL CONSIDERATIONS

APPLICATIONS

- PROTEIN BIOCHEMISTRY APPLICATION
- MICROPATTERING-BASED BIOMIMETIC APPLICATIONS
- CELL BIOLOGY APPLICATIONS
- SINGLE MOLECULE LOCALIZATION

courtesy: see last slide

microsurgery

human lung tissue (histology)

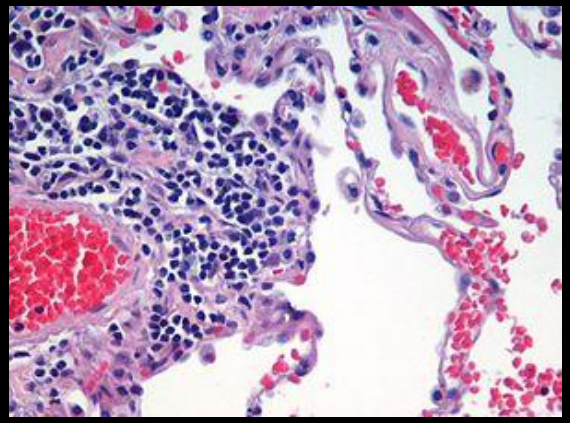

cell migration
(phase contrast)

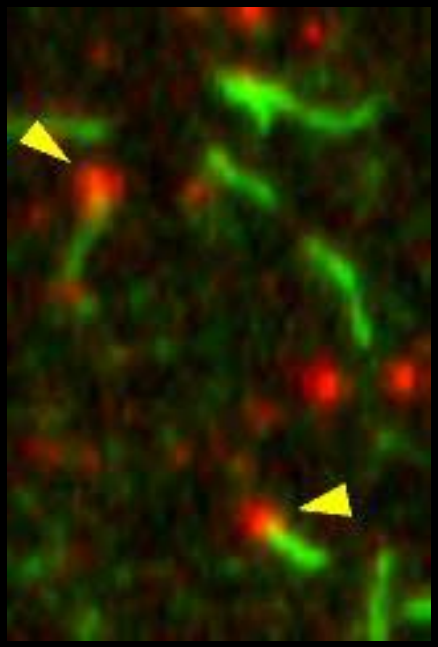

individual molecules
formin, actin
(TIRFM)

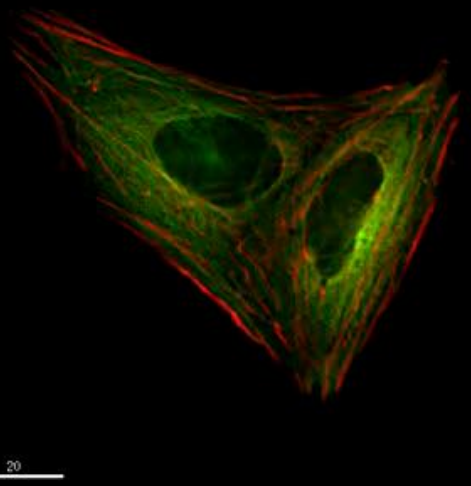

mitosis
actin, microtubule
(confocal)

World Cell Race
2011

CLASSICAL LIMIT OF RESOLUTION

1873 DIFFRACTION LIMIT THEORY
(Ernst Abbe, Carl Zeiss)

OBJECT (POINT) → IMAGE (3D STRUCTURE)

BOTTLENECK OF LM/FM:
RESOLUTION IS INTRINSICALLY LIMITED BY THE WAVE NATURE OF LIGHT.

$$d_{xy} = 0.61\frac{\lambda}{NA} \sim 200\ nm$$

$$d_z = 2n\frac{\lambda}{(NA)^2} \sim 800\ nm$$

$$NA = nsin\alpha$$

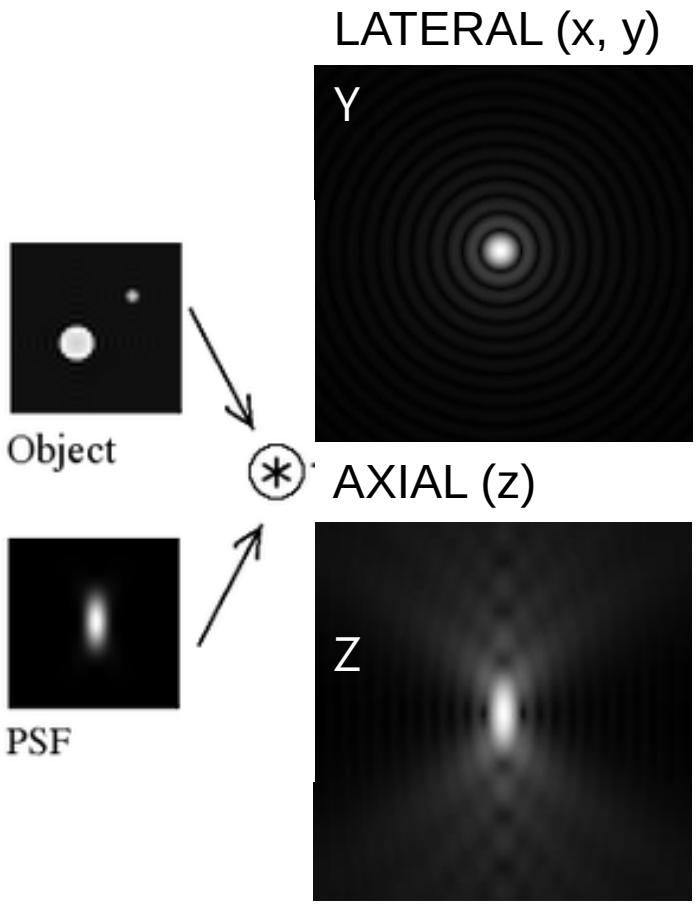

$$image = object \otimes PSF + noise$$

CLASSICAL LIMIT OF RESOLUTION

1873 Abbe's diffraction limit

Ernst Abbe memorial, Jena

2014 breaking the diffraction limit

Nobel prize in Chemistry

Stefan Hell, Eric Betzig and William Moerner

"for the development of super-resolved fluorescence microscopy"

http://www.nobelprize.org/nobel_prizes/chemistry/laureates/2014/

„SUPER-RESOLUTION" FLUORESCENCE MICROSCOPY

FLUORESCENCE MICROSCOPE (1911)
CONFOCAL MICROSCOPY (1961)

- illumination through pinhole, conjugate planes (~500 – 600 nm)

Minsky, M. Microscopy Apparatus. US Patent 3,013,467 (1961)

TOTAL INTERNAL REFLECTION FLUORESCENCE MICROSCOPY (1981)

- evanescent wave illumination (~ 100 nm)

Axelrod, D. Cell-substrate contacts illuminated by total internal reflection fluorescence. J. Cell Biol. 89, 141–145 (1981)

STIMULATED EMISSION MICROSCOPY (2000)

- PSF engineering, stimulated emission of fluorescence (~ tens of nm)

Klar, T. A., Jakobs, S., Dyba, M., Egner, A. & **Hell, Stefan.** W. Fluorescence microscopy with diffraction resolution barrier broken by stimulated emission. *Proc. Natl Acad. Sci. USA* **97**, 8206–8210 (2000)

SINGLE MOLECULE LOCALIZATION MICROSCOPY (STORM, PALM) (2006)

- phototransformable fluorophores, Gaussian fit (~ tens of nm)

Betzig, Eric. *et al*. Imaging intracellular fluorescent proteins at nanometer resolution. *Science* **313**, 1642–1645 (2006)

Rust, M. J., Bates, M. & Zhuang, X. Sub-diffractionlimit imaging by stochastic optical reconstruction microscopy (STORM). *Nature Methods* **3**, 793–796 (2006)

Dickson RM, Cubitt AB, Tsien RY and **Moerner William** (1997) On/off blinking and switching behaviour of single molecules of green fluorescent protein. Nature 388:355-358.

STRUCTURED ILLUMINATION MICROSCOPY (2008)

- sequential illumination through a rotating grid (~ 100 nm)

Karadaglic, D. and Wilson, T. Image formation in structured illumination wide-field fluorescence microscopy. Micron 39: 808-818 (2008).

TOTAL INTERNAL REFLECTION MICROSCOPY

E. J. Ambrose
Nature 1956

„In order to study the contacts formed between cells and solid surfaces, it is possible to make use of the **slight penetration of light waves into the less dense medium when totally internally reflected** at the glass/water interface."

nonfluorescent, evanescent light scattering from cells

crease with duration of the heating, the radioactive yield into purified *p*-nitro benzoic acid is likely to be much less than 44 per cent in the second case.

After purification, and removal of the activity from the carboxyl group, the overall yield was about 70 per cent by weight (17 per cent by activity), the specific activity being 230 mc./gm.

Further studies on the use of this material are in progress. A detailed account of the method will be published elsewhere.

J. E. S. Bradley

Physics Department,
Middlesex Hospital Medical School,
London, W.1.
Sept. 7.

[1] Ingold, C. K., Raisin, C. G., and Wilson, C. L., *Nature*, **134**, 734 (1934).
[2] Best, A. P., and Wilson, C. L., *J. Chem. Soc.*, 239 (1946).
[3] Gold, V., and Satchell, D. P. N., *J. Chem. Soc.*, 3609 (1955).
[4] Gold, V., and Satchell, D. P. N., *J. Chem. Soc.*, 3622 (1955).
[5] Koizumi, M., and Titani, T., *Bull. Chem. Soc. Japan*, **13**, 318 (1938).

A Surface Contact Microscope for the study of Cell Movements

The importance of the contacts formed by moving cells in controlling their behaviour has been clearly shown in the phenomenon of contact guidance described by Weiss[1] and in contact inhibition described by Abercrombie and Heaysman[2].

In order to study the contacts formed between cells and solid surfaces, it is possible to make use of the slight penetration of light waves into the less dense medium when totally internally reflected at a glass/water interface. The apparatus used for these studies is illustrated in Fig. 1. Light from an intense source *S* (compact-source mercury arc) passes through the slit *T* and strikes the upper surface *A* of the 60°-prism. A cell suspension in water is mounted between an ordinary microscope slide and a coverslip and is sealed with immersion oil on the upper face of the prism (Fig. 2). The incident light now strikes the upper surface of the glass slide at an angle greater than the critical angle and is totally internally reflected at the glass/water interface. In reality the beam penetrates the less dense medium slightly, as shown diagrammatically in Fig. 3(*a*). If a cell of refractive index greater than water is moving on

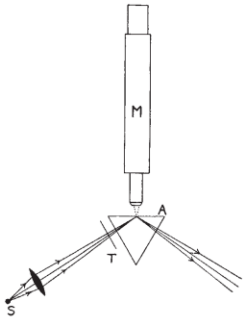

Fig. 1

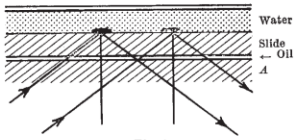

Fig. 2

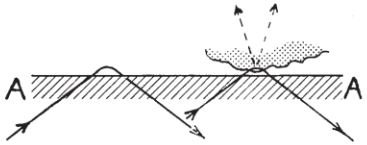

Fig. 3

the surface (Fig. 3(*b*)), those portions which make close contact with the surface of the glass will enter the penetrating beam and will scatter the light, owing to the presence of minute inhomogeneities in their structure.

When seen from above, through the microscope *M*, the field appears completely dark, provided that the incident light beam has been carefully shielded and the prism faces are clean. But those regions of the moving cells which are in close contact with the glass are brightly illuminated. In addition, the actual contours of the cell surface can be explored by changing the angle of the incident beam. With increasing angle, the degree of penetration of the incident beam is decreased so that the areas of the cell which are illuminated are reduced, eventually to those regions which are almost in molecular contact with the glass surface.

The effect is particularly well illustrated in the case of a filamentous mould kindly provided by Dr. R. J. Goldacre. As the mould moves forward along the glass, bright waves of light can be seen to move rapidly along its length, which are due to continuous changes in the points of adhesion between the lower surface of the mould and the glass surface. Apart from its biological application, the microscope may prove to be generally useful for the study of a number of phenomena, particularly those connected with the forces of cohesion between surfaces.

I am grateful to Prof. A. Haddow for his interest and encouragement in this work. This investigation has been supported by grants to the Chester Beatty Research Institute (Institute of Cancer Research: Royal Cancer Hospital) from the British Empire Cancer Campaign, Jane Coffin Childs Memorial Fund for Medical Research, the Anna Fuller Fund and the National Cancer Institute of the National Institutes of Health, U.S. Public Health Service.

E. J. Ambrose

Chester Beatty Research Institute,
Institute of Cancer Research:
Royal Cancer Hospital,
London, S.W.3.
July 27.

[1] Weiss, P., "Principles of Development" (Henry Holt and Co., New York, 1939).
[2] Abercrombie, M., and Heaysman, J. E. M., *Exp. Cell Res.*, **5**, 111 (1953); **6**, 293 (1954).

http://www.nature.com/nature/journal/v178/n4543/abs/1781194a0.html

TOTAL INTERNAL REFLECTION FLUORESCENCE MICROSCOPY

D. Axelrod
Journal of Cell Biology 1981

„The new method is an application … and extension to fluorescence of the total internal reflection micorscope illumination system introduced by Ambrose."

Cell-Substrate Contacts Illuminated by Total Internal Reflection Fluorescence

DANIEL AXELROD
Biophysics Research Division and Department of Physics, University of Michigan, Ann Arbor, Michigan 48109

ABSTRACT A technique for exciting fluorescence exclusively from regions of contact between cultured cells and the substrate is presented. The technique utilizes the evanescent wave of a totally internally reflecting laser beam to excite only those fluorescent molecules within one light wavelength or less of the substrate surface. Demonstrations of this technique are given for two types of cell cultures: rat primary myotubes with acetylcholine receptors labeled by fluorescent α-bungarotoxin and human skin fibroblasts labeled by a fluorescent lipid probe. Total internal reflection fluorescence examination of cells appears to have promising applications, including visualization of the membrane and underlying cytoplasmic structures at cell-substrate contacts, dramatic reduction of autofluorescence from debris and thick cells, mapping of membrane topography, and visualization of reversibly bound fluorescent ligands at membrane receptors.

The regions of contact between a tissue culture cell and a solid substrate are of considerable interest in cell biology. These regions are obvious anchors for cell motility (1), loci for aggregation of specific membrane proteins (2–4), and convergence points for cytoskeletal filaments (2, 5, 6). Described here is a fluorescence microscope method for selectively visualizing specific molecules in cell-substrate contact regions while avoiding fluorescence excitation of the cell interior liquid medium and cellular debris. Other potential applications of this method include viewing fluorescence-marked receptors at very low cell surface concentrations, cytoplasmic filaments in thick cells, and fluorescent agonists that bind reversibly to the cell membrane.

The new method is an application of total internal reflection fluorescence (TIRF) to cellular microscopy and is an extension to fluorescence of the total internal reflection microscope illumination system introduced by Ambrose (7) to detect light scattered at cell-substrate contacts. TIRF microscopy utilizes a light beam in the substrate that is obliquely incident upon the substrate liquid interface at an angle greater than the critical angle of refraction. At this angle, the light beam is totally reflected by the interface. However, an electromagnetic field called the "evanescent wave" does penetrate into the liquid medium. The evanescent wave propagates parallel to the surface with an intensity I that decays exponentially with perpendicular distance z from the surface:

$$I = I_o \exp(-z/d) \quad (1)$$

The characteristic exponential decay depth d is:

$$d = \frac{\lambda}{4\pi n_2}\left(\frac{\sin^2\theta}{\sin^2\theta_c} - 1\right)^{-1/2}, \quad (2)$$

where n_1 = refractive index of the substrate; n_2 = refractive index of the liquid medium; θ_c = the critical angle of incidence $= \sin^{-1} n_2/n_1$; θ = the angle of incidence, $\theta > \theta_c$; and λ = the wavelength of incident light in vacuum. The decay depth d decreases with increasing θ. Except for θ close to θ_c (where $d \to \infty$), d is on the order of λ or smaller. I_o, the intensity of the evanescent wave at $z = 0$, is on the order of the incident light intensity except for angles of incidence very near the critical angle (8). Therefore, for most experimental configurations, a fluorescent molecule located in the evanescent wave at $z = 0$ will be excited with roughly the same efficiency as it would if it were located in the incident beam.

A fluorescent molecule located close to the surface in the evanescent wave can become excited and emit fluorescence; molecules much farther away will not be excited. The efficiency of excitation decays exponentially according to Eqs. 1 and 2. For typical experiments described here, identical fluorescent molecules located at 1, 10, 100, and 1,000 nm from the surface will emit relative fluorescence intensities of 0.99, 0.92, 0.43, and 0.0002, respectively. For cells adhering to the surface, only fluorescent molecules at or near the cell surface in the regions of closest contact with the substrate will be excited significantly.

TIRF has been employed previously to study surface interactions in a variety of molecular systems, including solutions of fluorescein (9) and serum albumin (10, 11) at glass surfaces, and antibodies at antigen coated surfaces (12). More recently, TIRF has been combined with fluorescence photobleaching recovery and fluorescence correlation spectroscopy to study the surface adsorption/desorption kinetics of fluorescent macromolecules (13, 14) and viruses (15).

A completely unrelated transmitted illumination technique,

THE JOURNAL OF CELL BIOLOGY · VOLUME 89 APRIL 1981 141-145
© The Rockefeller University Press · 0021-9525/81/04/0141/05 $1.00

PHYSICAL PRINCIPLES OF TIRFM

TOTAL INTERNAL REFLECTION – CRITICAL ANGLE

SNELL'S LAW OF REFRACTION

$$n_1 sin\alpha_1 = n_2 sin\alpha_2$$

IF

$$\boldsymbol{n_1 > n_2}$$

THEN

$$\alpha_1 < \alpha_2$$

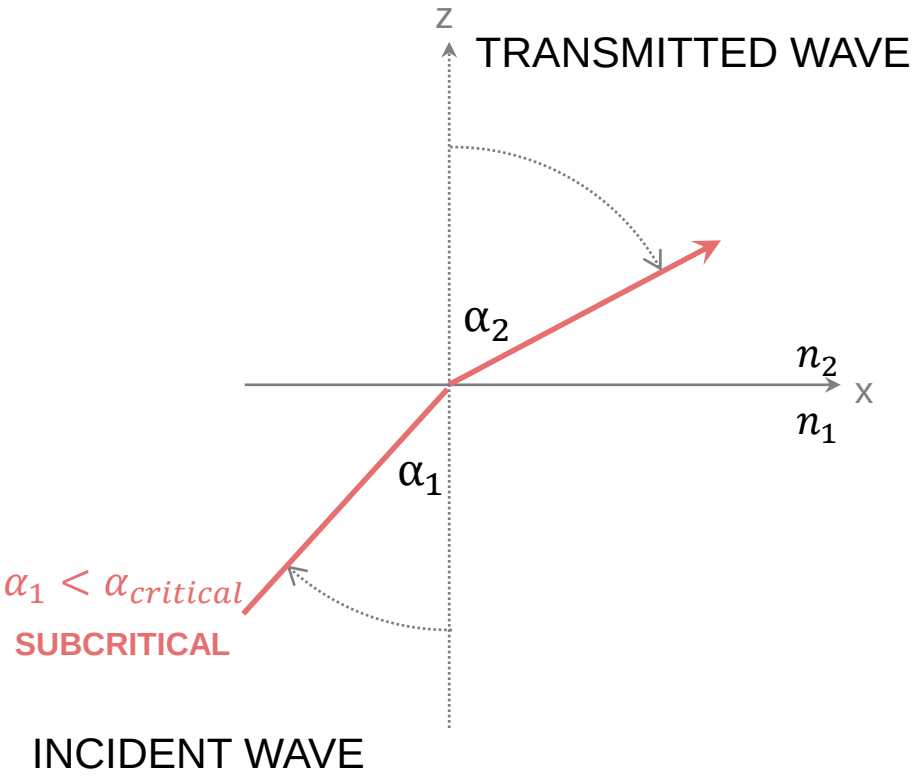

Notation:
1: incident wave/1st medium
2: transmitted wave/2nd medium

TOTAL INTERNAL REFLECTION – CRITICAL ANGLE

SNELL'S LAW OF REFRACTION

$$n_1 sin\alpha_1 = n_2 sin\alpha_2$$

IF

$$\boldsymbol{n_1 > n_2}$$

THEN

$$\alpha_1 < \alpha_2$$

CRITICAL ANGLE

$\alpha_{critical} \equiv \alpha_1$ when $\alpha_2 = 90^0$

$$\boldsymbol{\frac{n_1}{n_2} sin\alpha_{critical} = 1}$$

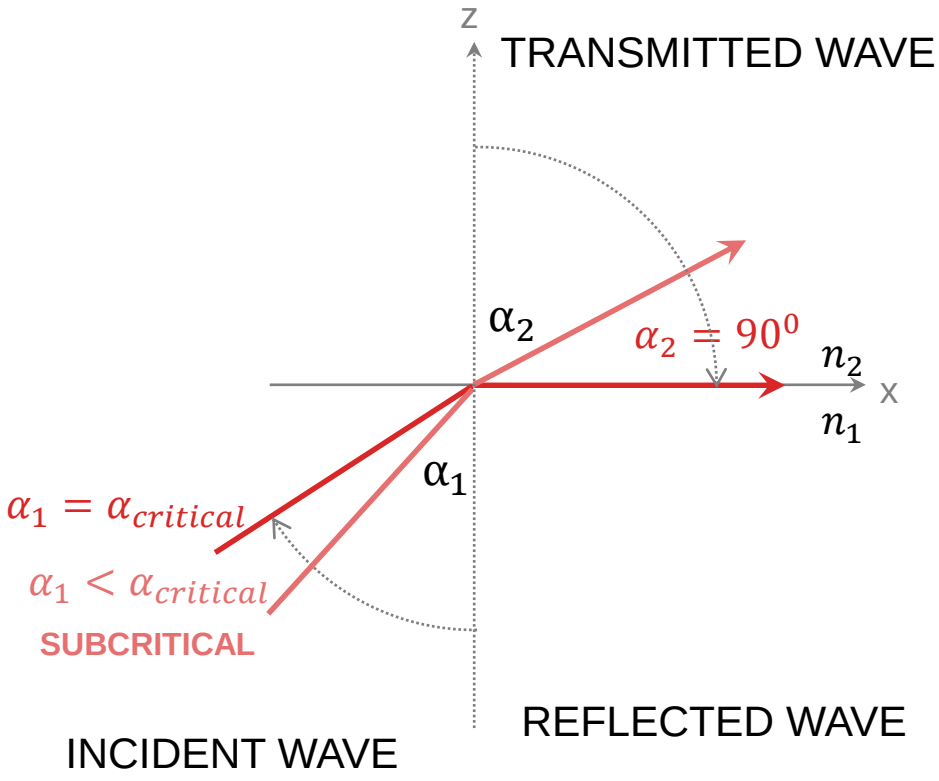

Notation:
1: incident wave/1st medium
2: transmitted wave/2nd medium

TOTAL INTERNAL REFLECTION – CRITICAL ANGLE

SNELL'S LAW OF REFRACTION

$$n_1 sin\alpha_1 = n_2 sin\alpha_2$$

IF

$$\boldsymbol{n_1 > n_2}$$

THEN

$$\alpha_1 < \alpha_2$$

CRITICAL ANGLE

$\alpha_{critical} \equiv \alpha_1$ when $\alpha_2 = 90^0$

$$\boldsymbol{\frac{n_1}{n_2} sin\alpha_{critical} = 1}$$

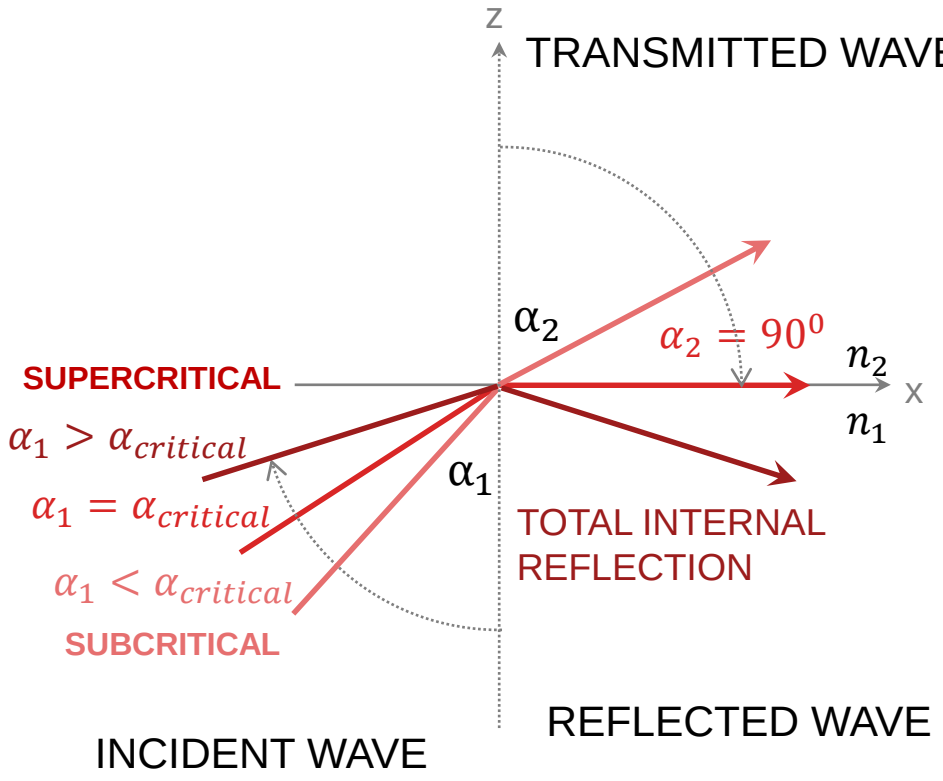

Notation:
1: incident wave/1st medium
2: transmitted wave/2nd medium

TOTAL INTERNAL REFLECTION – CRITICAL ANGLE

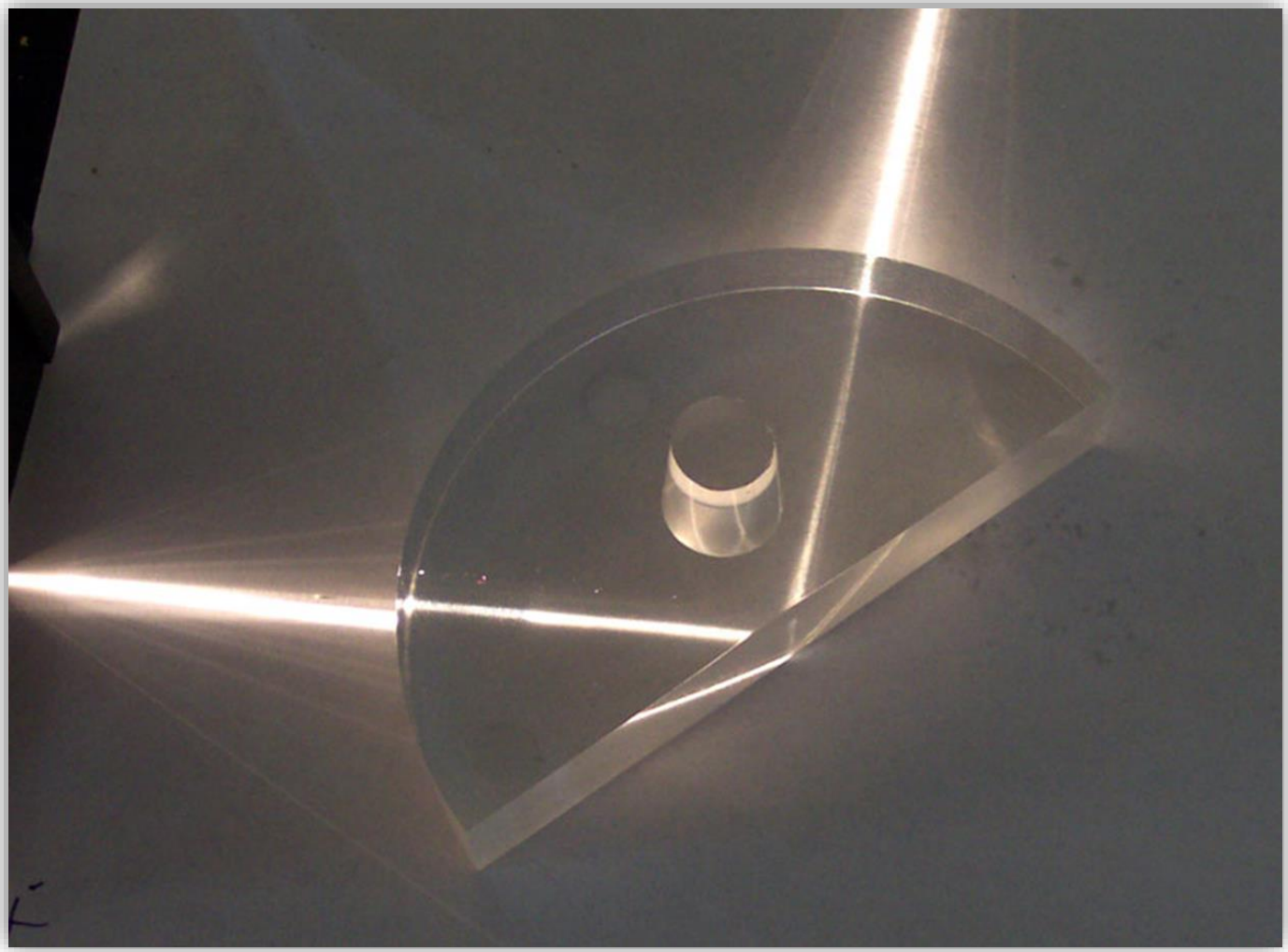

TOTAL INTERNAL REFLECTION – CRITICAL ANGLE

EVANESCENT WAVE

MONOCHROMATIC PLANE WAVE/XZ

INCIDENT

$$\vec{E}_1(\vec{r},t) = \vec{E}_1 \exp\left[i(\vec{k}_1\vec{r} - \omega t)\right]$$

TRANSMITTED

$$\vec{\mathbf{E}}_2(\vec{\mathbf{r}},\mathbf{t}) = \vec{\mathbf{E}}_2 \mathbf{exp}\left[\mathbf{i}\left(\vec{\mathbf{k}}_2\vec{\mathbf{r}} - \boldsymbol{\omega}\mathbf{t}\right)\right] =$$
$$= \vec{E}_2 \exp\left[i(k_2 sin\alpha_2 x + k_2 cos\alpha_2 z - \omega t)\right]$$

$$ik_2(sin\alpha_2 x + cos\alpha_2 z) = ik_2\left(\frac{sin\alpha_1}{n}x + i\sqrt{\frac{sin^2\alpha_1}{n^2} - 1}z\right)$$

IF $\alpha_1 = \alpha_c$, then $\vec{E}_2(\vec{r},t) =$

$$= \vec{E}_2 exp[i(k_2 x - \omega t)] \quad \boldsymbol{Z\ diappears}$$

IF $\alpha_1 > \alpha_c$, then $\vec{E}_2(\vec{r},t) =$

$$= \vec{E}_2 exp\left[i\left(k_2 \frac{sin\alpha_1}{n}x - \omega t\right)\right] \cdot exp\left[-k_2\sqrt{\frac{sin^2\alpha_1}{n^2} - 1}z\right]$$

The transmitted wave propagates parallel to the surface (x axis), as well as in the z direction, where it is attenuated exponentially.

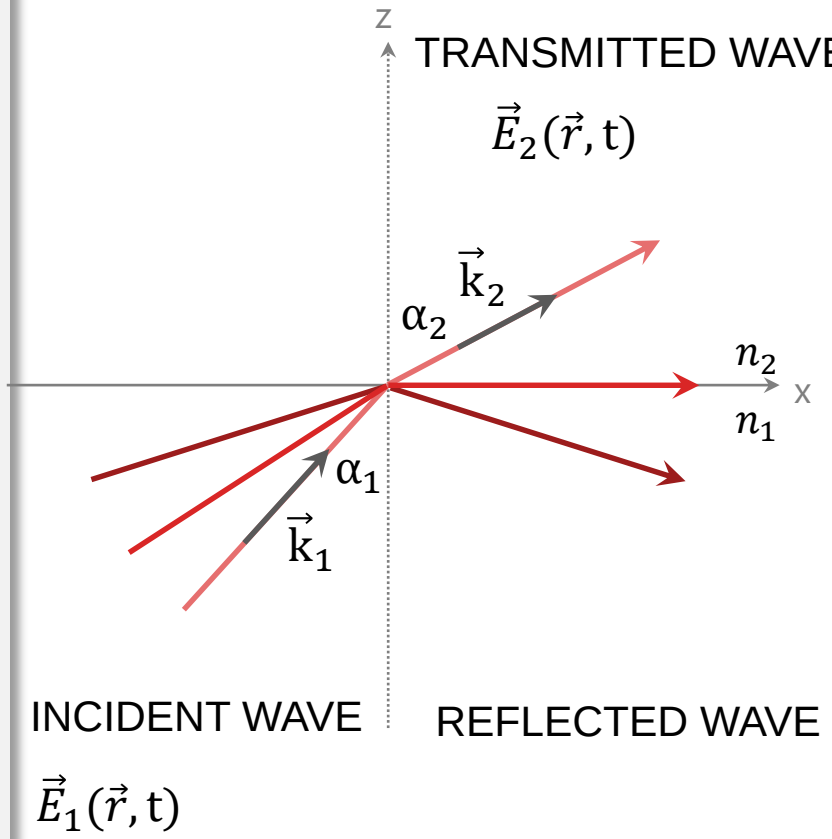

TOTAL INTERNAL REFLECTION – CRITICAL ANGLE

EVANESCENT WAVE

$$\vec{E}_{\text{evanescent}}(\vec{r}, t) =$$

$$\vec{E} exp[-k_2 \sqrt{\frac{sin^2\alpha_1}{n^2} - 1} z]$$

$$= \vec{E} exp\left[-\frac{2\pi}{\lambda}\frac{1}{n_2}\sqrt{sin^2\alpha_1 {n_1}^2 - {n_2}^2} z\right]$$

INTENSITY PROFILE

$$I(z) = \left|\vec{E}\right|^2 = \mathbf{I_0 exp}\left(-\frac{\mathbf{z}}{\mathbf{d}}\right)$$

WHERE

$$\mathbf{d} = \frac{\boldsymbol{\lambda}}{\mathbf{4\pi n_1}}\left(\mathbf{sin^2\alpha_1} - \left(\frac{\mathbf{n_2}}{\mathbf{n_1}}\right)^2\right)^{-\frac{1}{2}}$$

PENETRATION DEPTH/DECAY LENGTH

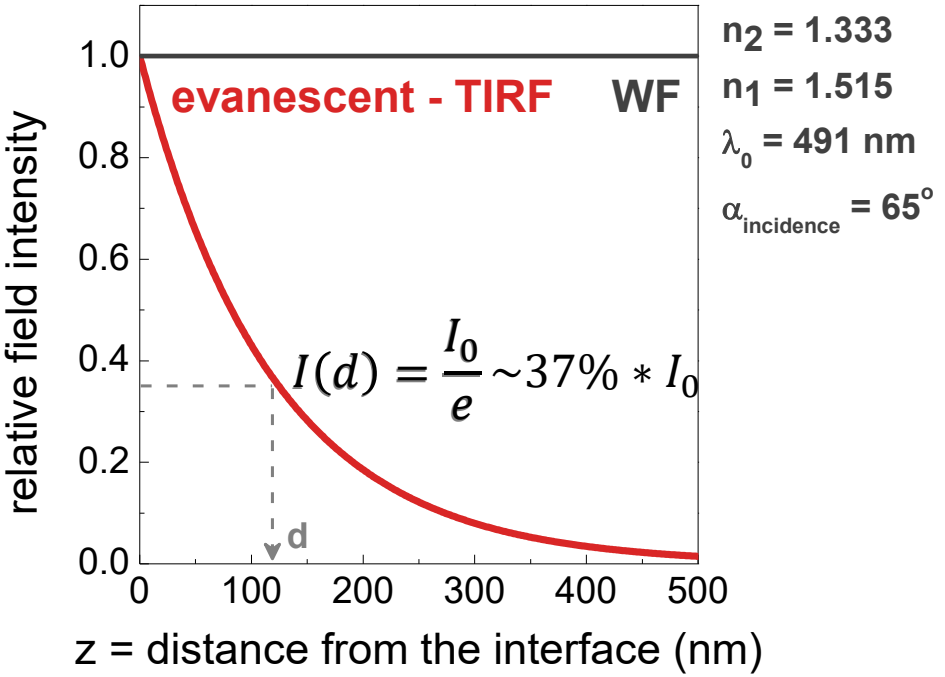

TOTAL INTERNAL REFLECTION – CRITICAL ANGLE

CRITICAL ANGLE

$$sin\alpha_{critical} = \frac{n_2}{n_1}$$

$\alpha_{critical}$ depends on the relative refractive index ratio of the two media. If the $n = n_2/n_1$ is small, the critical angle is shallow and TIR is easily achieved.

GLASS : WATER INTERFACE

$$\frac{n_2}{n_1} = 0.879$$

$$\alpha_{critical} = 61.62^o$$

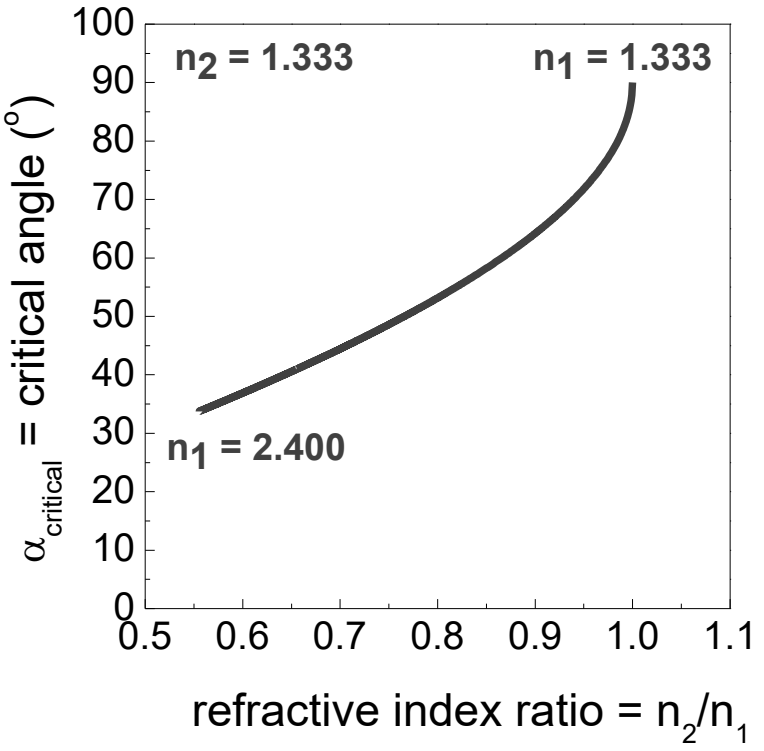

INFLUENCES ON THE „EVANESCENT" NATURE

$$d = \frac{\lambda}{4\pi n_1}\left(\sin^2\alpha_1 - \left(\frac{n_2}{n_1}\right)^2\right)^{-\frac{1}{2}}$$

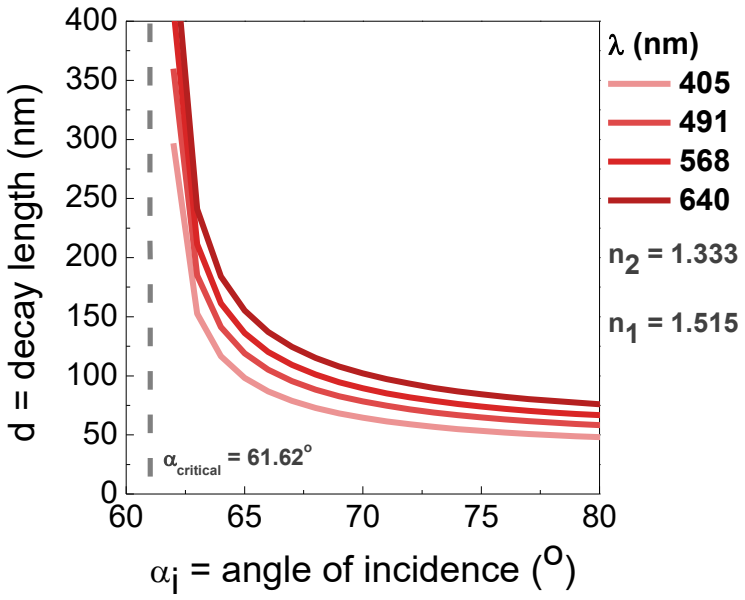

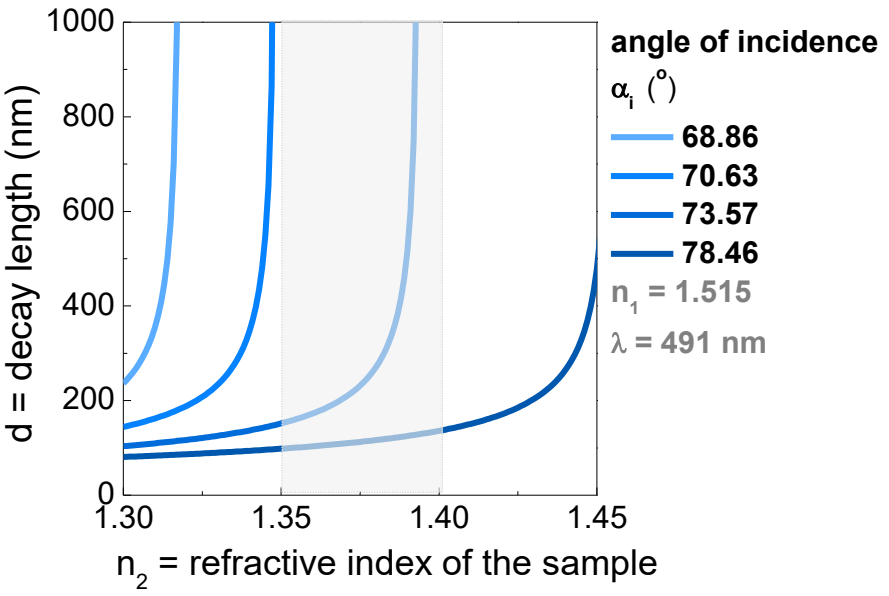

As the angle of incidence increases, the depth becomes narrower (resolution!)

$$\alpha_1 \rightarrow \alpha_{critical}: d \rightarrow \infty$$

As the wavelength decreases, the depth is narrower (resolution, co-localisation!)

As n_2 increases, the depth increases (resolution!).

As the angle of incidence increases, the sensitivity of the evanescent field to n_2 decreases.

TIRFM – EVANESCENT WAVE ILLUMINATION

EVANESCENT WAVE

- decays exponentially in intensity with increasing distance normal to the surface
- decay length (d) is in the order of the wavelength of the incident light (λ)
- selectively excites fluorophores very near to a solid surface (~ 100 nm)
- eliminates background fluorescence from out-of-focus planes, improves SNR

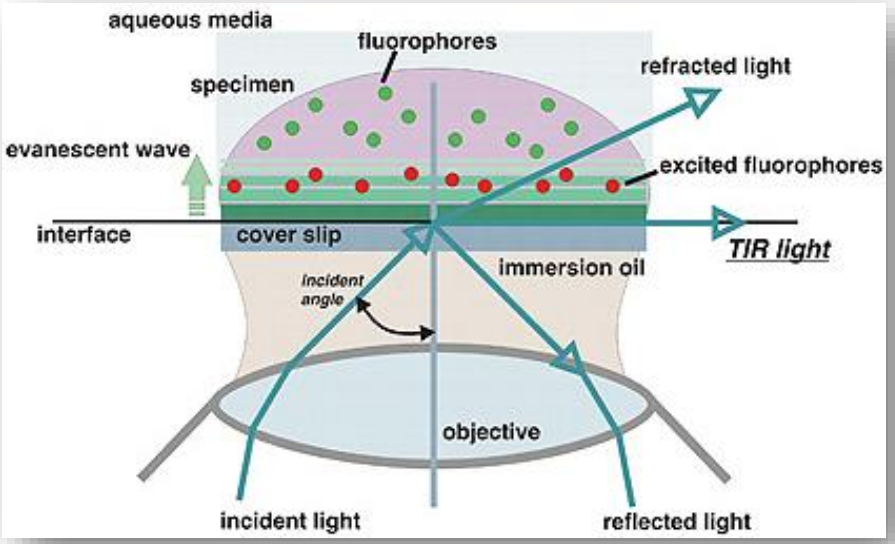

TIRFM, AS A NEAR-FIELD IMAGING METHOD PROVIDES A SURFACE-SELECTIVE ILLUMINATION AND RESOLUTION IMPROVEMENT DUE TO THE UNIQUE PROPERTIES OF THE EVANESCENT FIELD.

TIRFM APPLICATIONS

- **EXTRACELLULAR MATRIX STRUCTURE AND ASSEMBLY**
- **CELL-SURFACE CONTACT REGIONS**
  - focal adhesion dynamics
- **CELL MEMBRANE, CELL SURFACE RECEPTORS, ION CHANNELS**
- **EXOCYTOSIS, ENDOCYTOSIS**
- **SUBMEMBRANE CYTOSKELETAL DYNAMICS**
  - actin, microtubule cytoskeleton

TIRFM + COMBINED ADVANTAGES

- FRAP
- FRET
- AFM
- SINGLE MOLECULE LOCALIZATION TECHNIQUES (STORM, PALM)
- MICORPATTERNING
- MICORFLUIDCS

WF vs TIRF ILLUMINATION

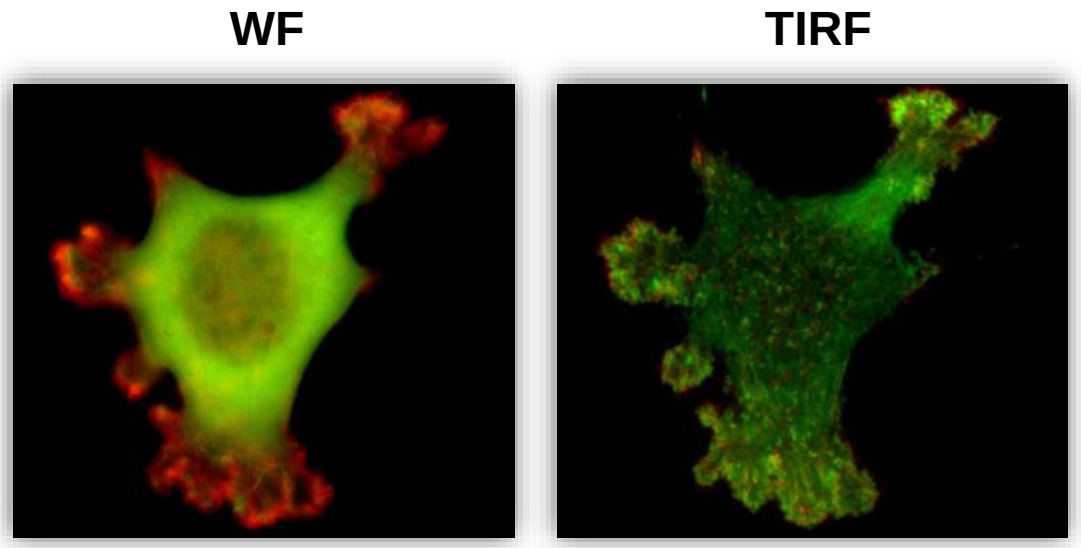

B16/F1 melanoma cell: EGFP-myosin (488 nm) mRFP-actin (514 nm)

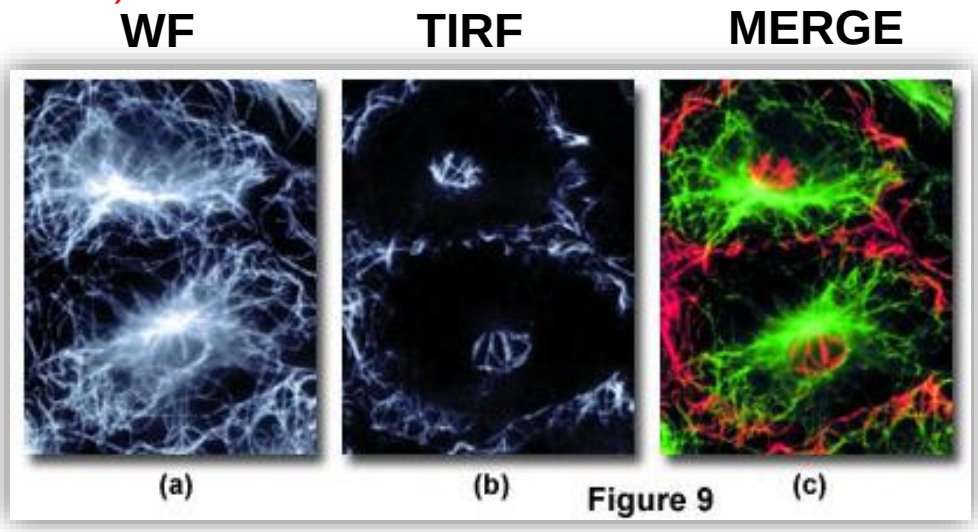

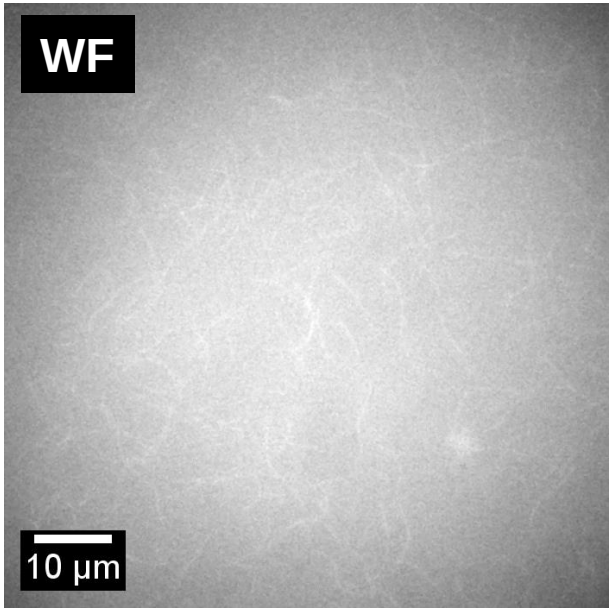

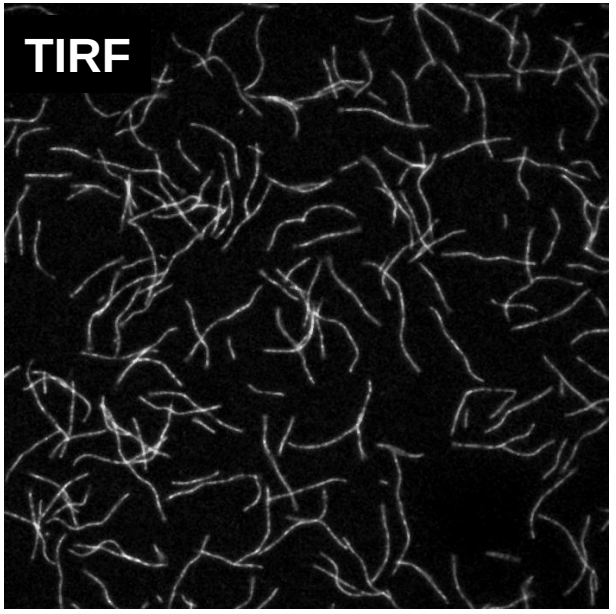

TRANSITION FROM WF TO TIRF

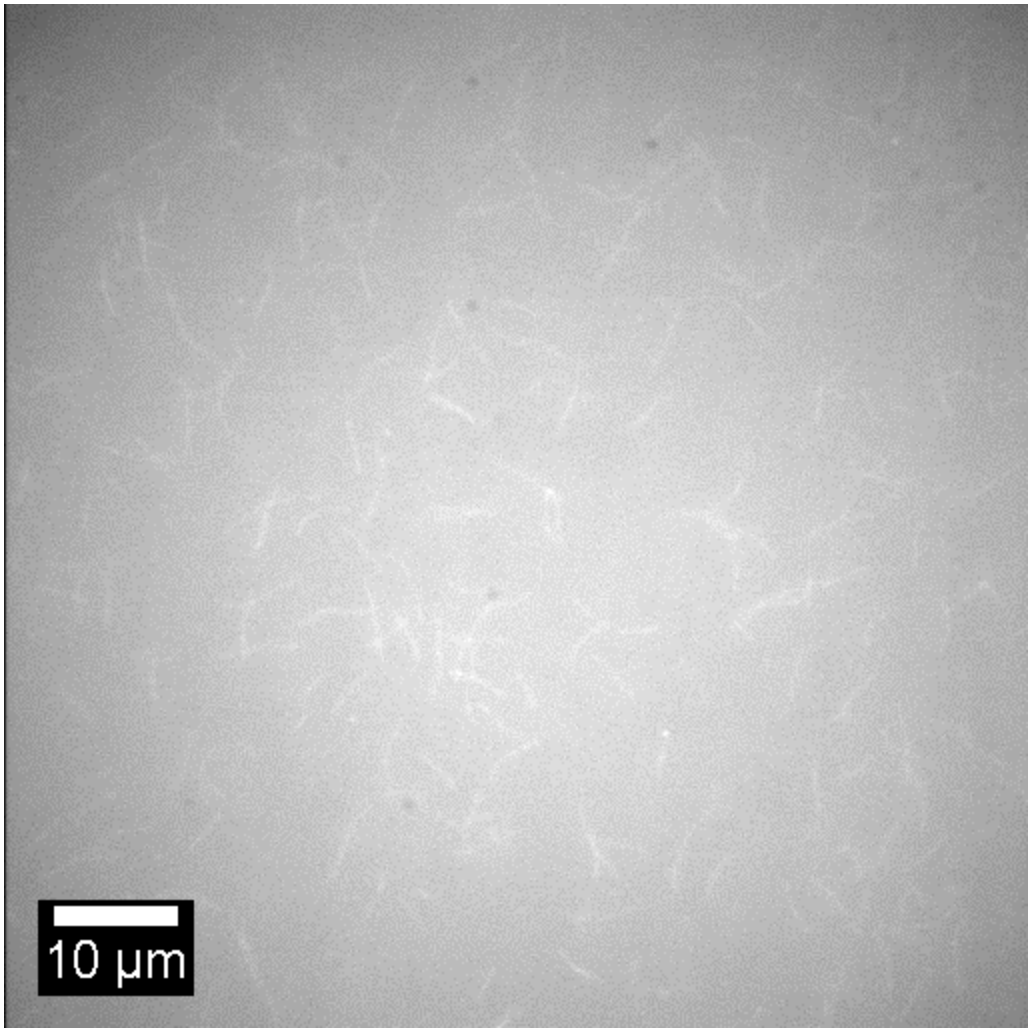

Olympus IX81 inverted microscope λ_{ex} = 491 nm, 60× 1.49 NA

TECHNICAL CONSIDERATIONS

HOW TO IMPLEMENT TIR PRINCIPLES INTO THE FLUORESCENCE MICROSCOPE?

- **REFRACTIVE INDEX RATIO**

THE REFRACTIVE INDEX OF THE 2ND MEDIUM HAS TO BE LOWER THAN THAT OF THE 1ST ONE

$n_1 > n_2$

$n_{glass(1)} = 1.515$

$n_{water(2)} = 1.333$

$n = \frac{n_2}{n_1} = 0.879$

$n_{cell(2)} = 1.36$

$n = \frac{n_2}{n_1} = 0.898$

- **CRITICAL ANGLE OF ILLUMINATION**

THE ANGLE OF INCIDENCE HAS TO BE LARGER THAN THE CRITICAL ANGLE

$\alpha_{incidence} > \alpha_{critical}$

for glass : water interface: $\alpha_{critical} = 61.62^o$

for glass : cell interface: $\alpha_{critical} = 63.86^o$

TIRFM SETUP

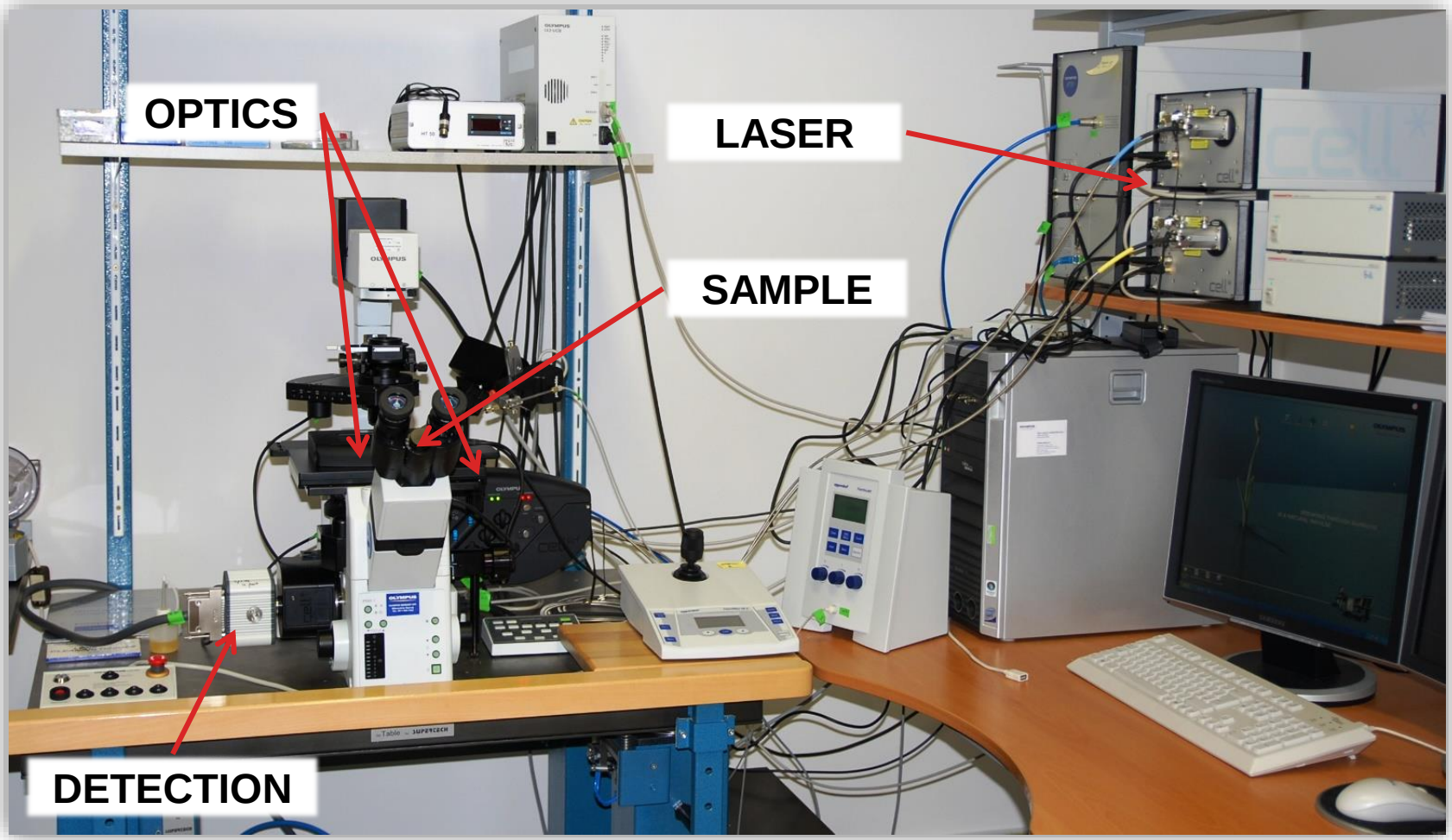

PRISM-BASED TIRFM

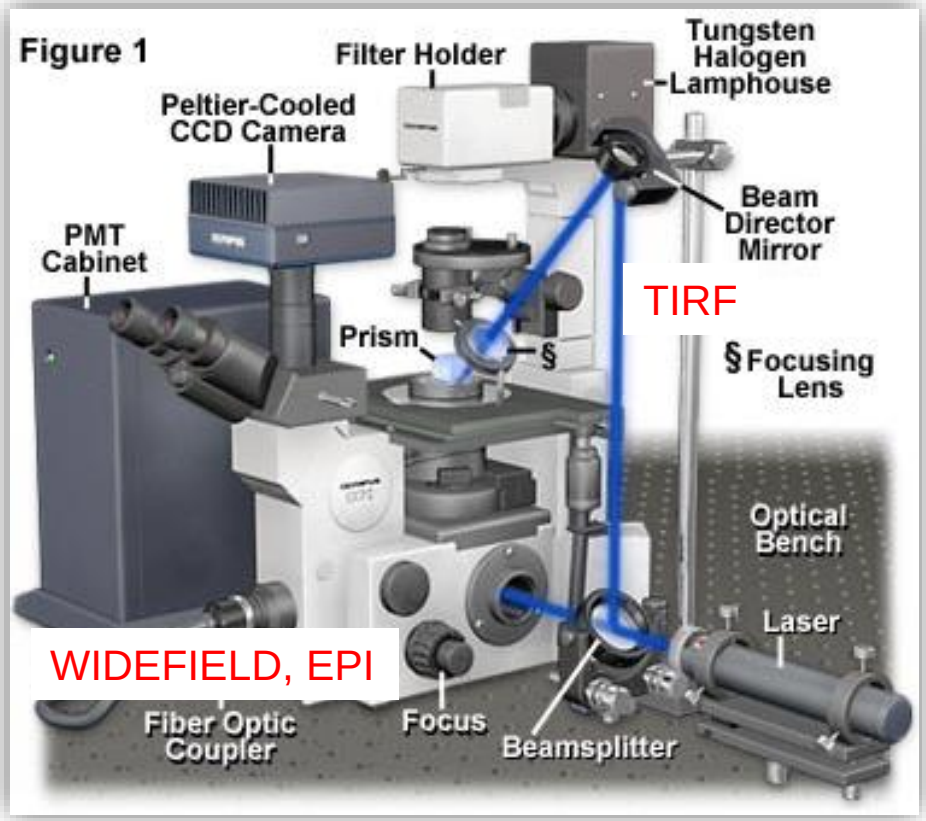

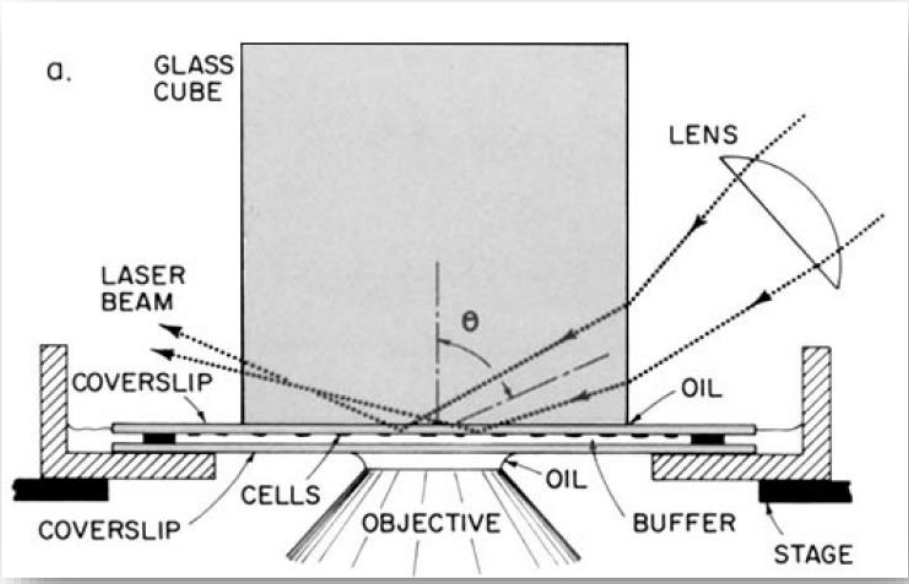

D. Axelrod Journal of Cell Biology 1981
http://www.olympusmicro.com/primer/techniques/fluorescence/tirf/tirfconfiguration.html

OBJECTIVE-BASED (PRISMLESS) TIRFM

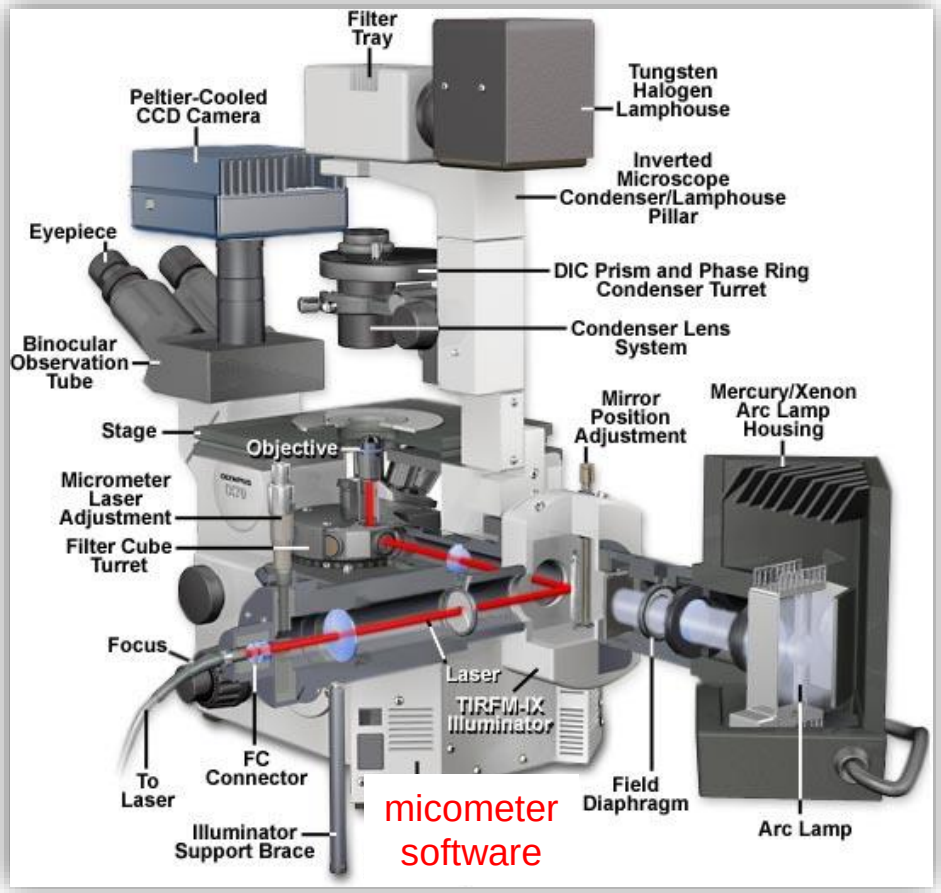

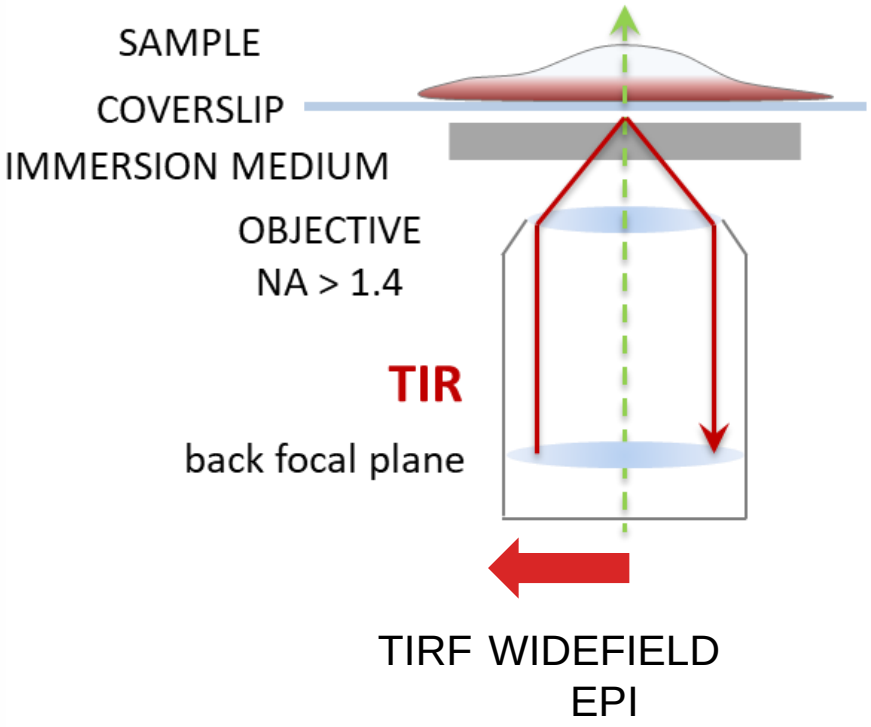

1001 arcú fehérjék: Fénymikroszkópiák a sejtszintű fehérjekutatásban (in Hungarian)

http://www.microscopyu.com/articles/fluorescence/tirf/tirfintro.html
http://www.olympusmicro.com/primer/techniques/confocal/applications/tirfmintro.html

LASER-BASED ILLUMINATION

LASER

- DIODE LASER
- DIODE PUMPED SOLID STATE LASER
- P up to 300 mW
- l = 405 - 640 nm

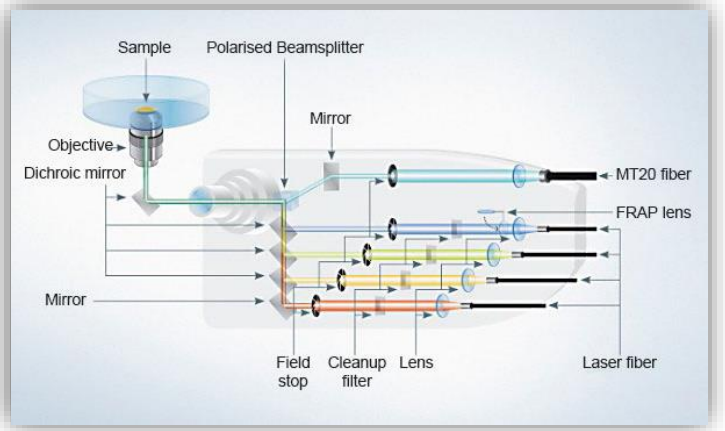

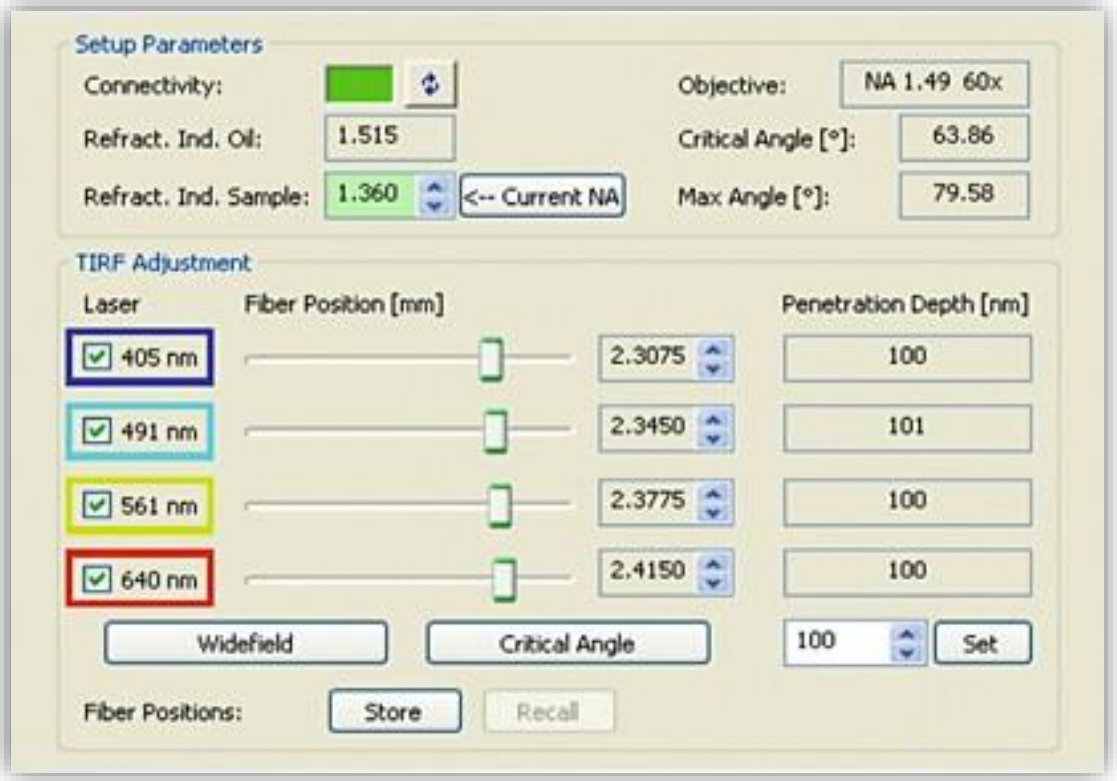

NUMERICAL APERTURE OF THE OBJECTIVE

glass : water interface

$n_{water\ (2)} = 1.333$

$n_{glass(1)} = 1.515$

$n_{immersion(1)} = 1.515$

$n_{critical} = 61.62^o$

$$\boldsymbol{NA(minimum)} = 1.515 * sin61.62^o = \mathbf{1.33}$$

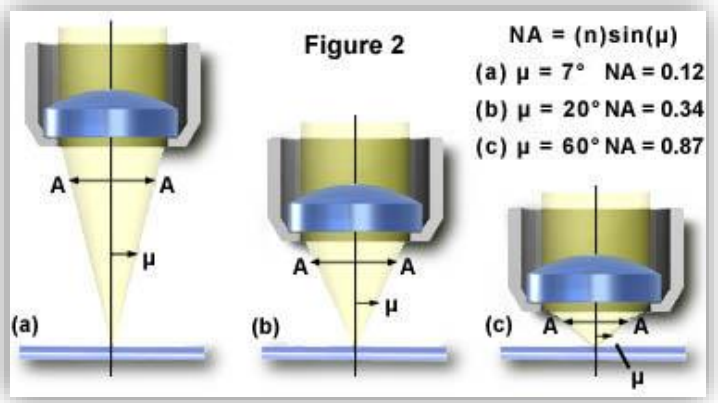

$$\boldsymbol{NA} \uparrow \rightarrow \boldsymbol{WD} \downarrow$$

glass : cell interface

$n_{cell(2)} = 1.38$

$n_{glass(1)} = 1.515$

$n_{immersion(1)} = 1.515$

$n_{critical} = 65.63^o$

$$\boldsymbol{NA(minimum)} = 1.515 * sin65.63^o = \mathbf{1.38}$$

$\boldsymbol{NA} \geq \mathbf{1.4}$!

micro.magnet.fsu.edu/primer/anatomy/numaperture.html

OBJECTIVE-BASED (PRISMLESS) TIRFM

	WD (mm)	NA	n_1 immersion	n_2 cell	critical angle (°)	maximum angle (°)	utilized NA fraction
plan apochromatic	-	1.4	1.515	1.38	65.63	67.53	0.02
UAPON 150xTIRF	0.08	1.45	1.515	1.38	65.63	73.15	0.07
APON 60XTIRF UAPON 100xTIRF	0.1 0.1	1.49	1.515	1.38	65.63	79.57	0.11
APON 100XTIRF	0.08	1.65 *	1.788	1.38	50.51	67.34	0.27

* special immersion oil and glass coverslip are needed

The excitation light has to pass through the portion of the numerical aperture cone that is greater than 1.38.

Being on the edge gives less flexibility.

AVAILABLE NUMERICAL APERTURE MARGIN

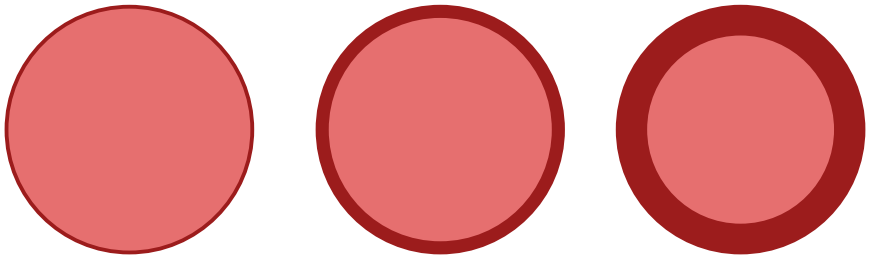

NA = 1.4
0.02

NA = 1.45
0.07

NA = 1.65
0.27

AVAILABLE NUMERICAL APERTURE MARGIN

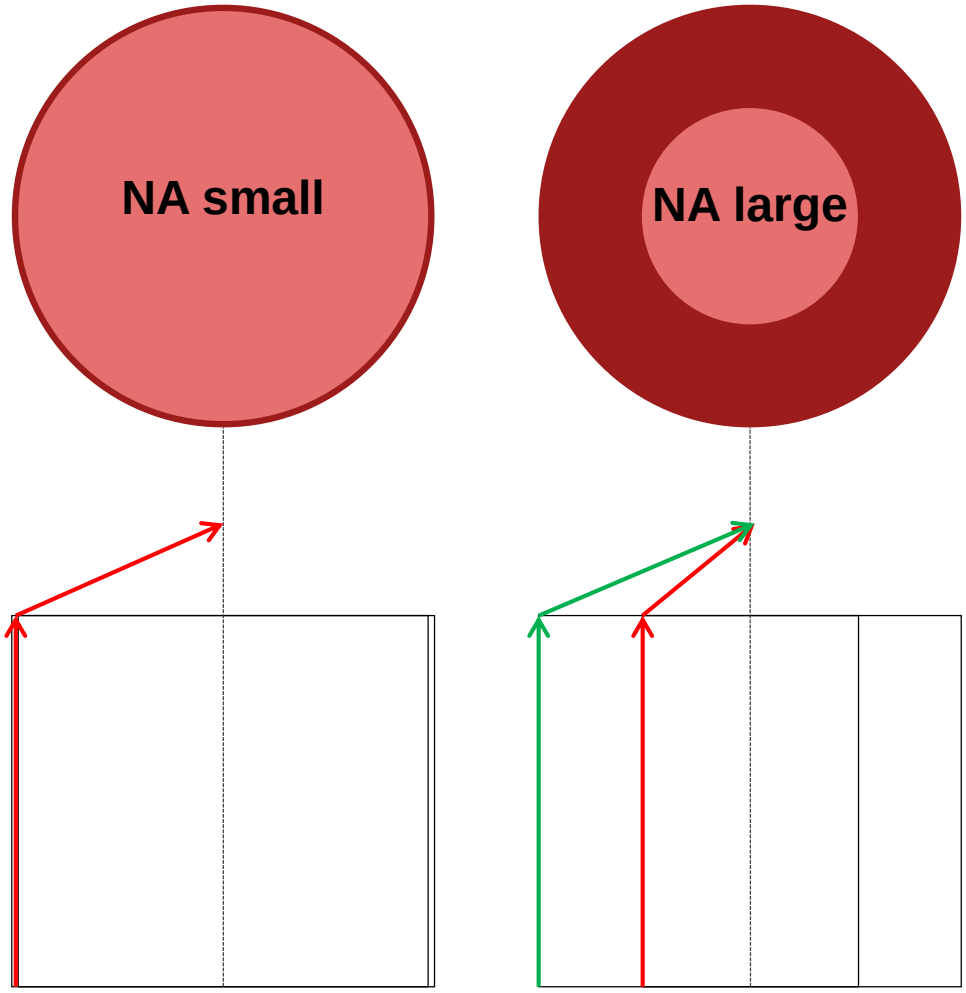

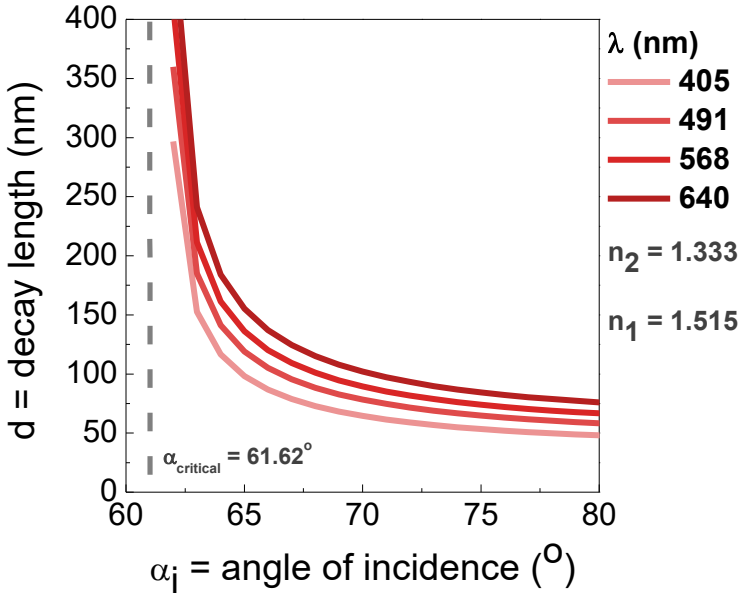

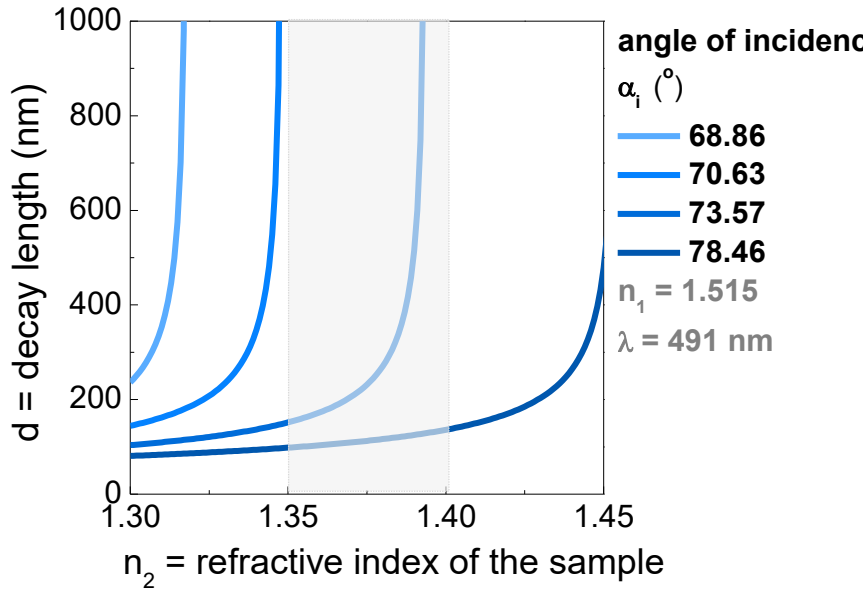

PRISM vs. OBJECTIVE-BASED TIRFM

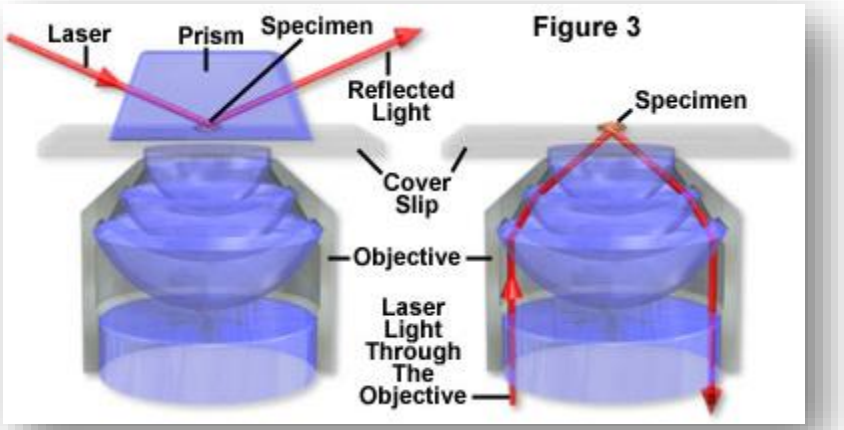

	PRISM-BASED TIRFM	OBJECTIVE-BASED TIRF
SYSTEM SETUP, ALIGMENT, MAINTENANCE	-	+
ANGLE OF INCIDENCE	+	-
ACCESS TO THE SAMPLE	-/+	+
LASER SAFETY	-	+
OBJECTIVE NEEDS	high working distance	high NA

http://www.microscopyu.com/articles/fluorescence/tirf/tirfintro.html
http://www.olympusmicro.com/primer/techniques/confocal/applications/tirfmintro.html

SAMPLE PREPARATION

SAMPLE (cells, proteins, …)
- fluorescently labeled, no restriction of usable fluorphores (!available wavelength, and filter set)
- oxigen scavenger system
- low refractive index medium

ENVIRONMENT
- immersion
- incubator
- autofocus

FLOW CELL
- manual / microfluidics

SURFACE CHEMISTRY
- poly-L-lysine (PLL)
- collagen/fibronectin
- PLL-g-PEG
- streptavidine-biotin
- NEM-myosin

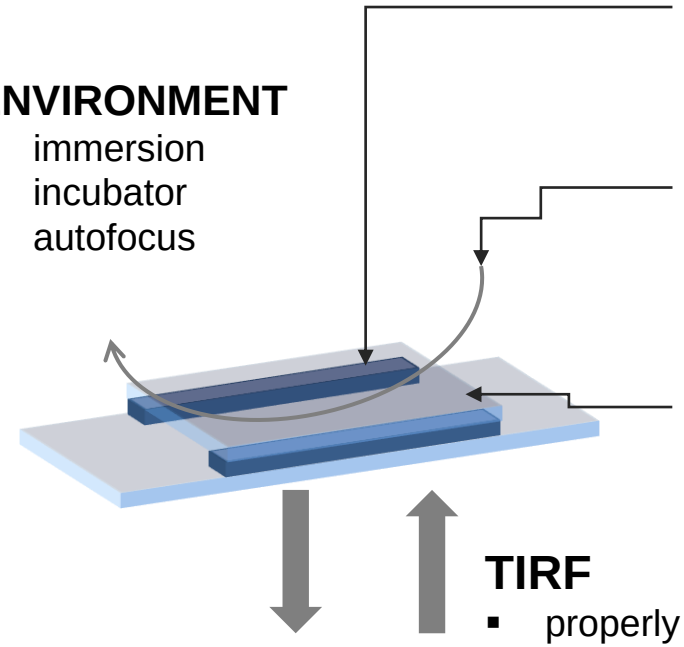

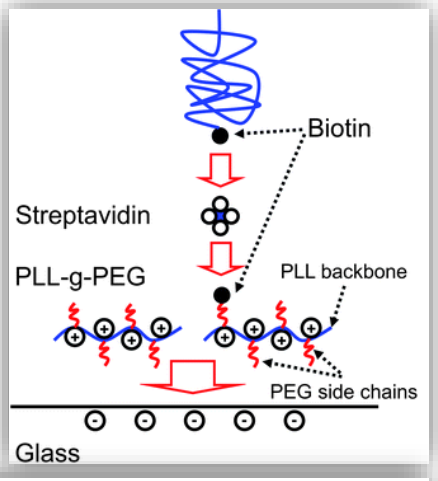

TIRF
- properly aligned laser beam
- no optical imperfections
- properly mounted coverslip (no tilt!)

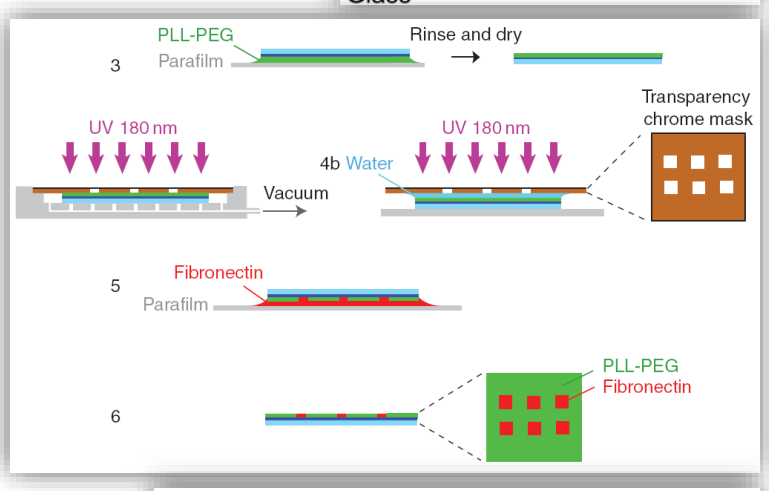

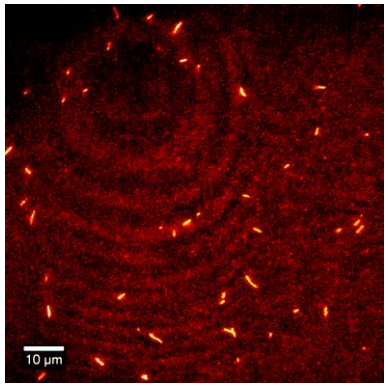

- interference fringes
- inhomogeneous field

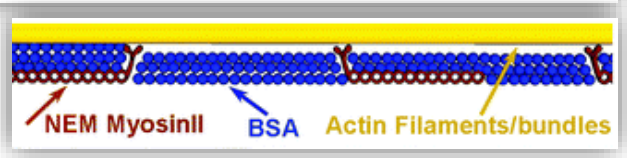

Azioune et al. Lab on a Chip 2009
Reymann AC. et al. Nature Materials 2010

TIRFM – PROTEIN BIOCHEMISTRY

TIRFM IN STUDYING CYTOSKELETAL POLYMER DYNAMICS

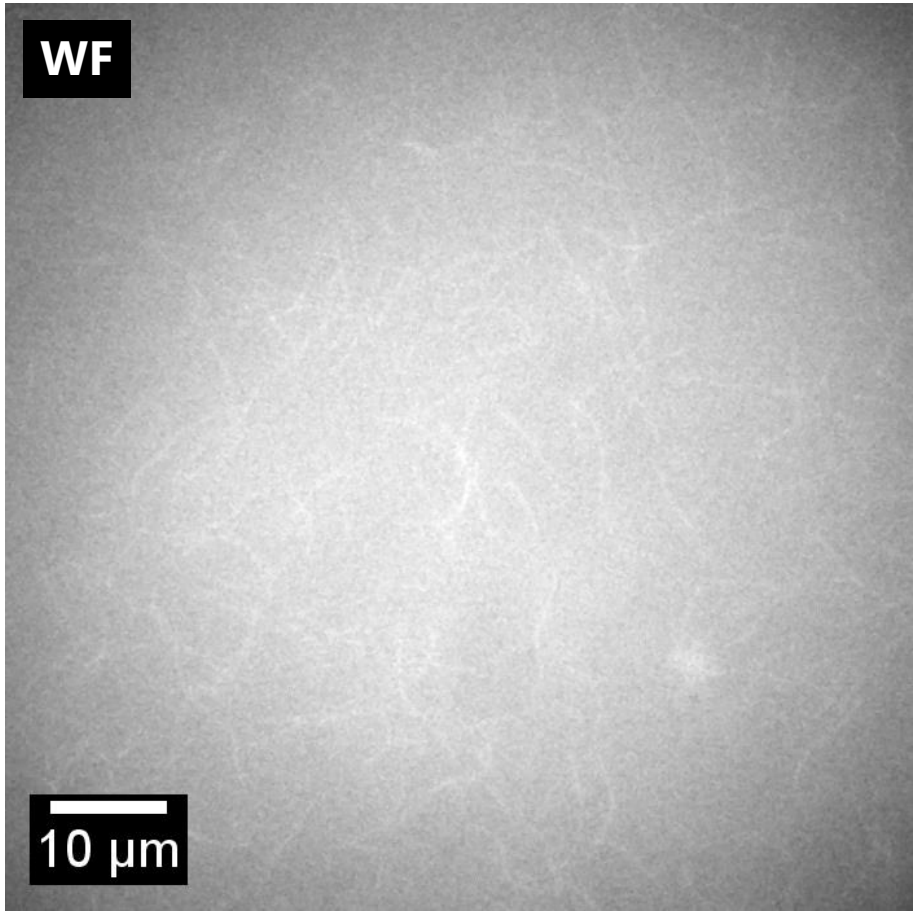

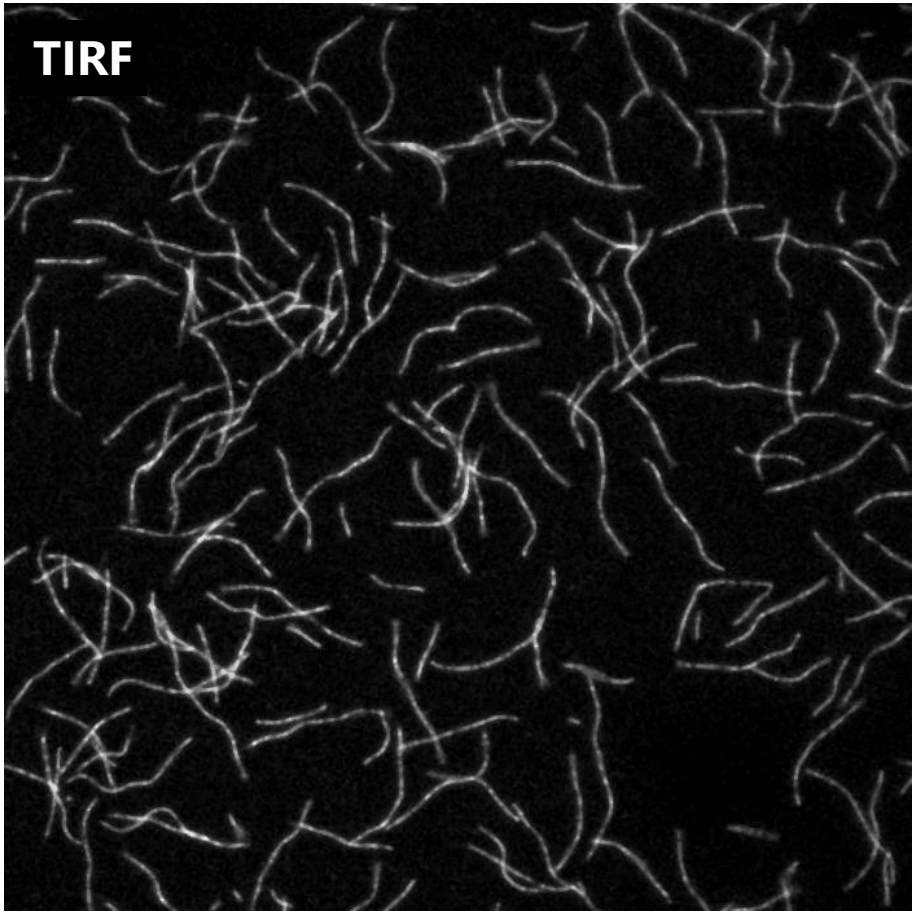

ACTIN BIOCHEMISTRY

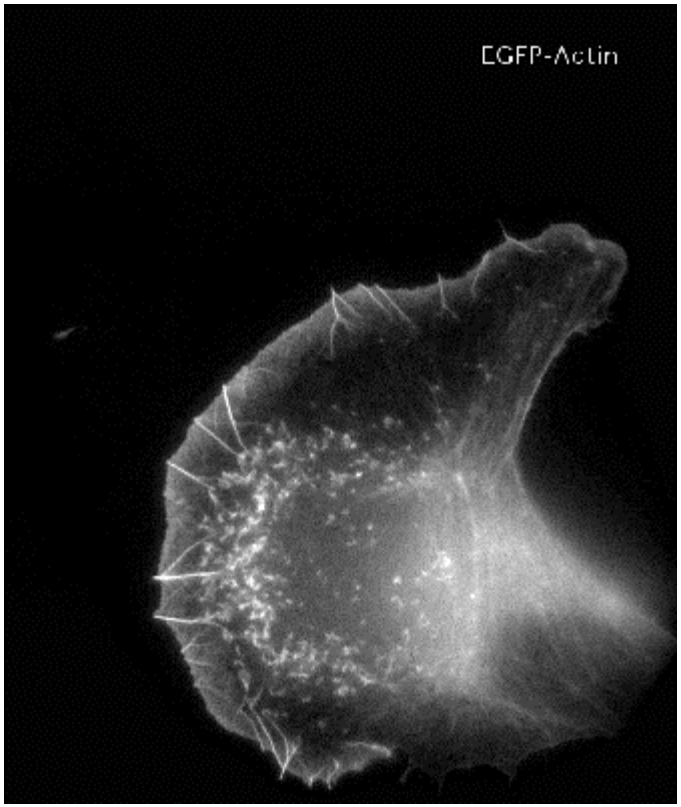

Courtesy: Klemens Rottner, Helmholtz Centre for Infection Research

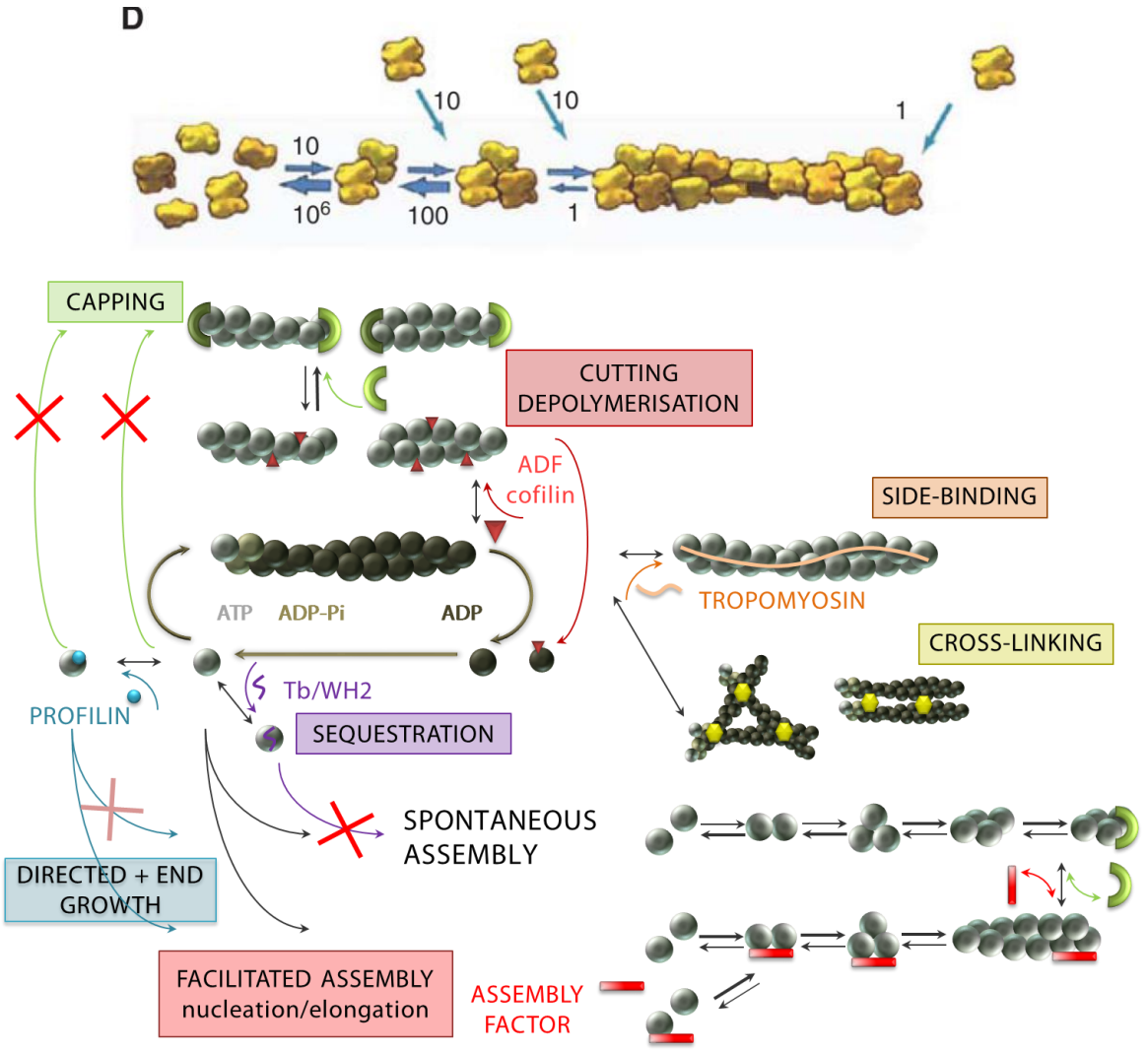

Pollard, T. D. *J. Cell Biol.* (1986), Pollard, T. D *Perspectives in Biology* (2016) adapted from Bugyi B., Carlier MF (2010) Annual Rev. in Biophysics, Renault L. Bugyi B. Carlier MF. *Trends in CB* 2008

ACTIN BIOCHEMISTRY

SPONTANEOUS ACTIN ASSEMBLY

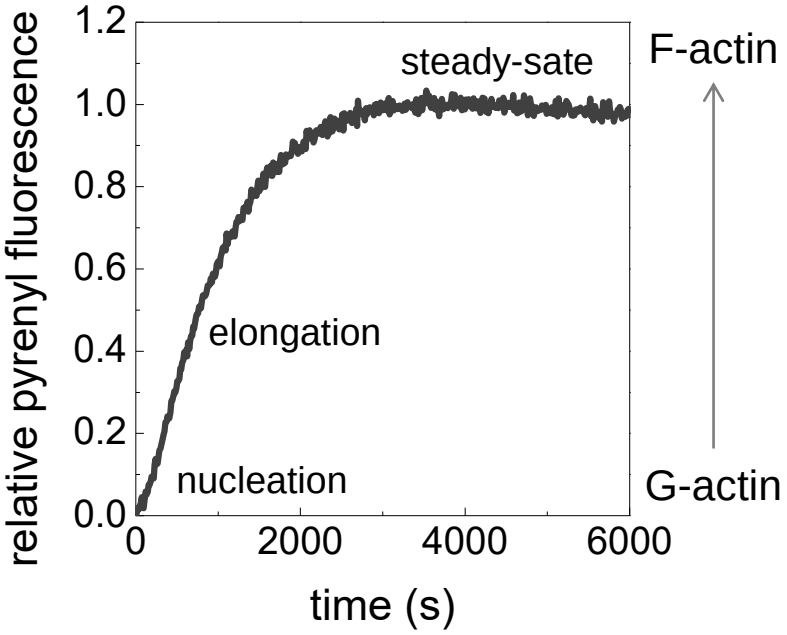

$$v = k_+[G_0 - c_c][F] - k_-[F]$$

ACTIN BIOCHEMISTRY

SPONTANEOUS ACTIN ASSEMBLY

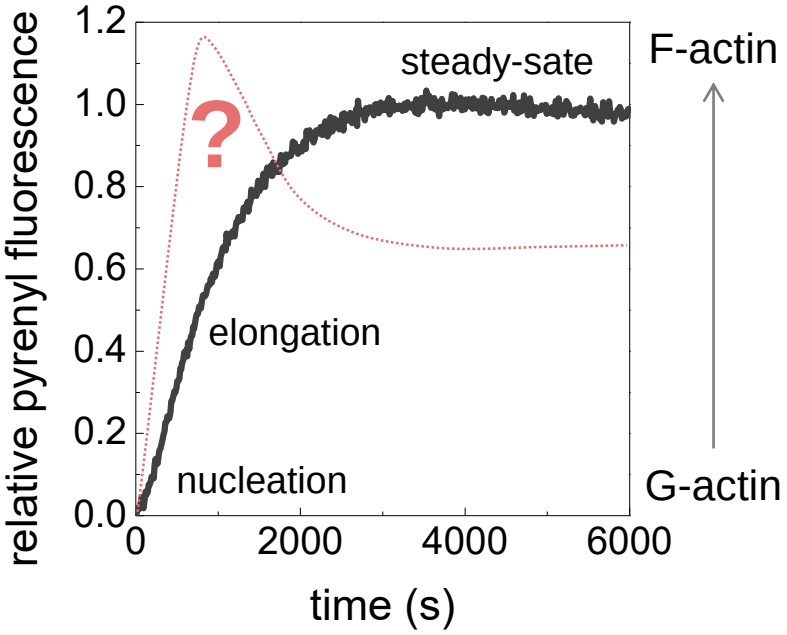

$$v = k_+[G_0 - c_c][F] - k_-[F]$$

STUDYING THE DYNAMIC BEHAVIOUR OF ACTIN
DIRECT „OBSERVATION" OF ABPs ACTIVITIES

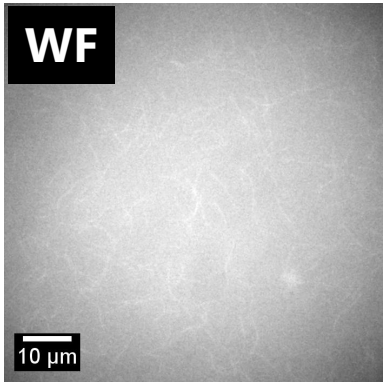

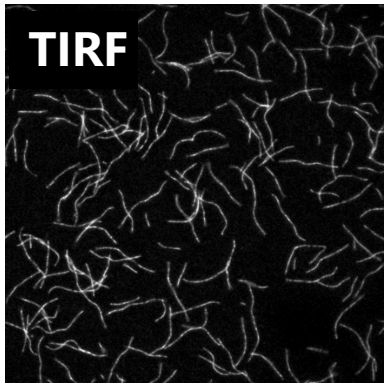

OBJECTIVE BASED TIRFM

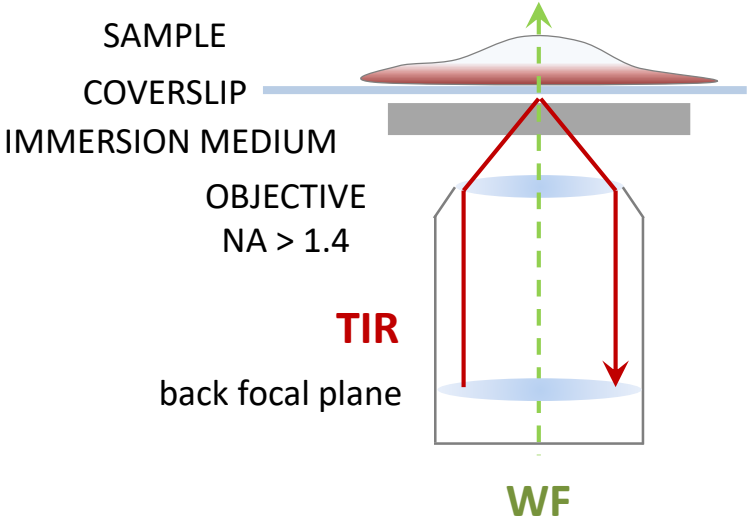

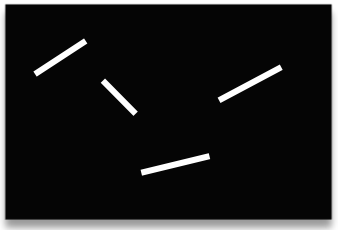

SPONTANEOUS ACTIN DYNAMICS
$k_+, k_-, [G], [F]$

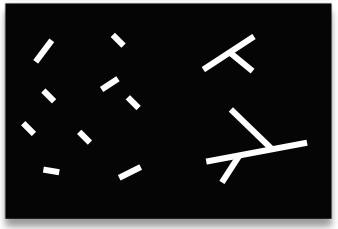

NUCLEATION FACTORS
$[F], k_+, k_-$
e.g. formins, Arp2/3 complex

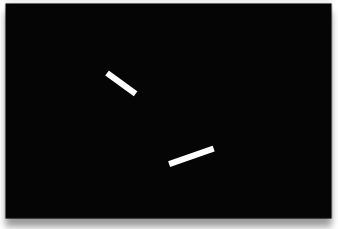

SEQUESTRATORS
$[G], [F]$
e.g. WH2 domain proteins

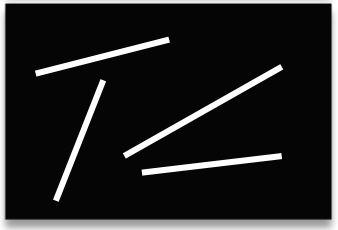

ELONGATION/CAPPING FACTORS
k_+, k_-
e.g. formins, VASP, CP

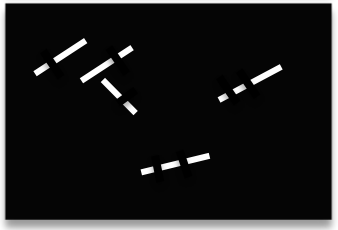

FILAMENT BINDING
$k_+, k_-, [F]$
severing, stabilization

1001 arcú fehérjék: Fénymikroszkópiák a sejtszintű fehérjekutatásban (in Hungarian)

ACTIN BIOCHEMISTRY

SPONTANEOUS GROWTH OF ACTIN FILAMENTS

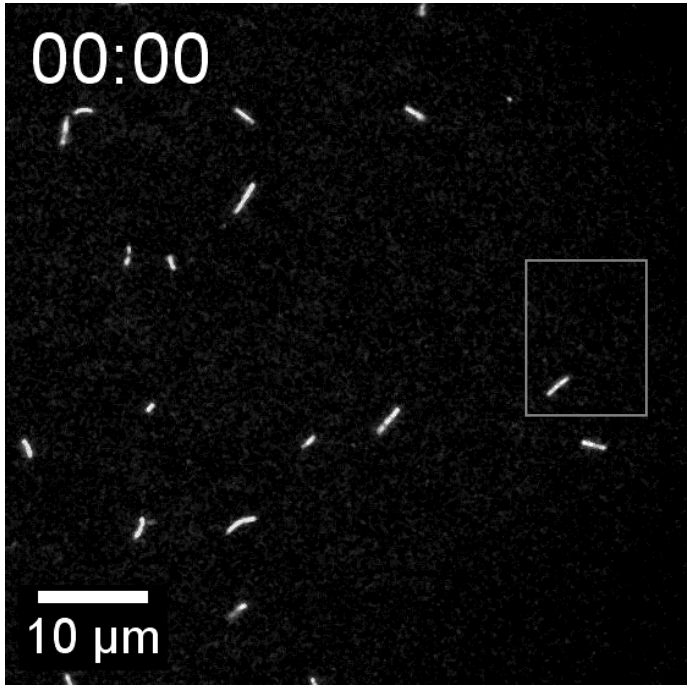

time = min : s
AlexaNHS488-ACTIN (10 % LABELED)
491 nm 60xNA1.45
t = 100 ms, I = 10% (P = 15 mW)
HamamatsuCCD

- POLYMER GROWTH RATE

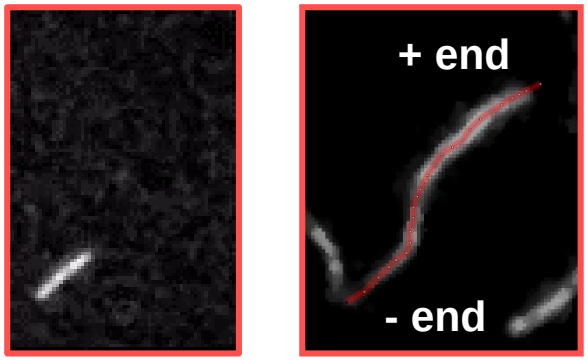

KYMOGRAPH

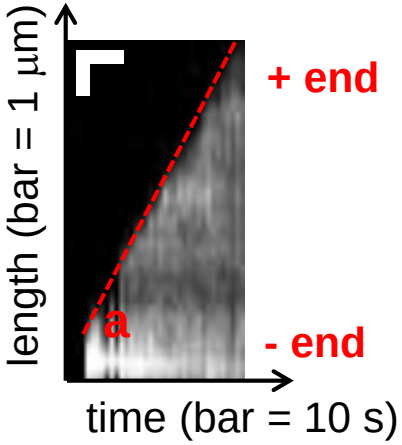

$$v_{elongation} = tan\alpha = \frac{\Delta length(\mu m)}{\Delta time\ (s)} = \frac{\Delta length * 370(su)}{\Delta time\ (s)}\ \left(\frac{\boldsymbol{su}}{\boldsymbol{s}}\right)$$

$$v_{elongation} = k_+[G - c_c] \rightarrow k_+ = 11\ \mu M^{-1}s^{-1}$$

ACTIN BIOCHEMISTRY

- **FILAMENT NUCLEATION**

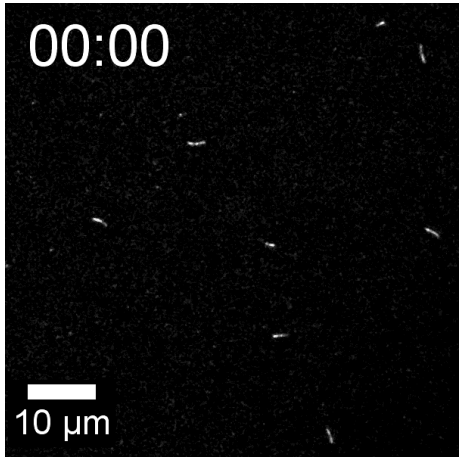

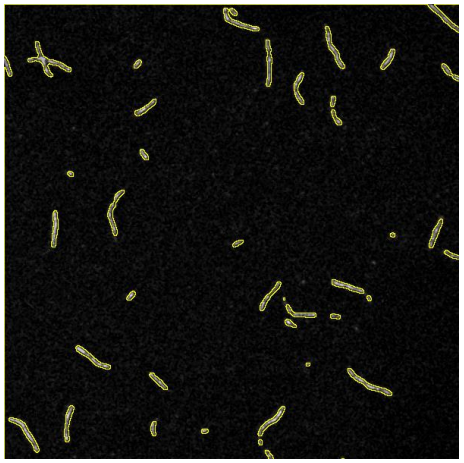

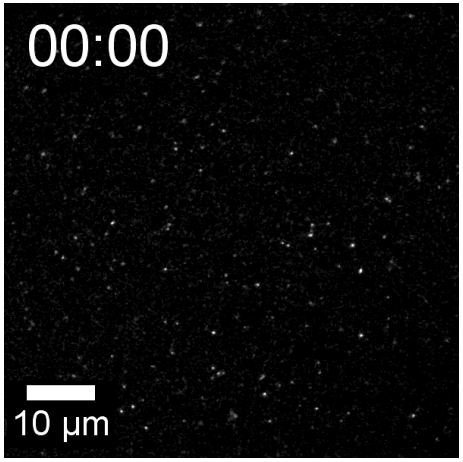

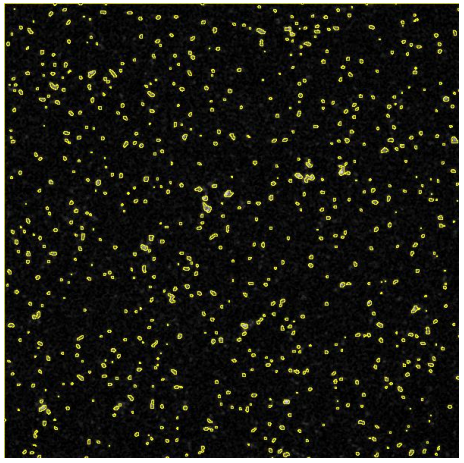

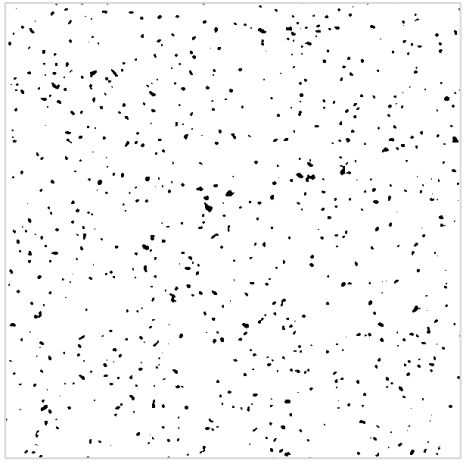

ACTIN BIOCHEMISTRY

- **FILAMENT DISASSEMBLY**

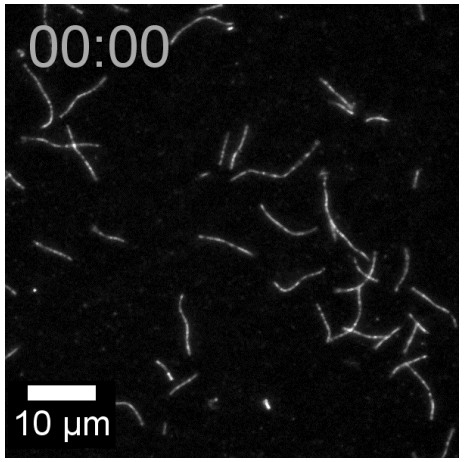

- **FILAMENT MORPHOLOGY**

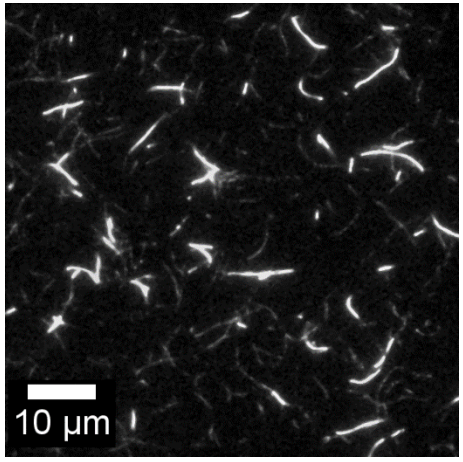

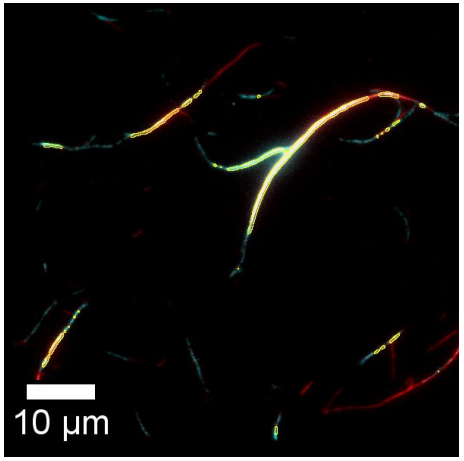

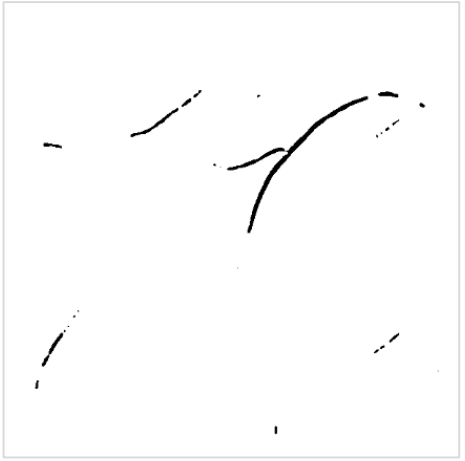

PRINCIPAL ORGANIZATION OF THE ACTIN AND MICROTUBULE CYTOSKELETON IN NEURONS

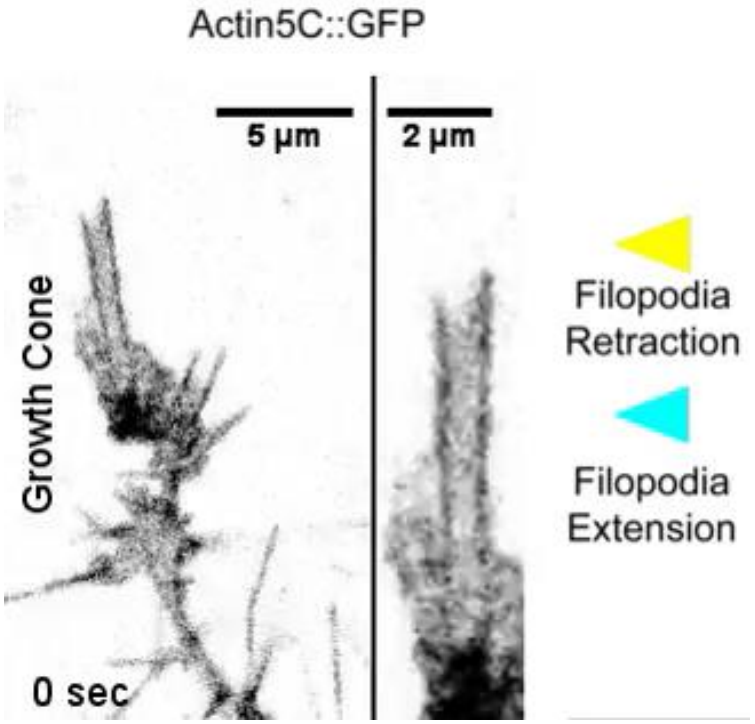

Growth cone dynamics in *Drosophila* primary neuron

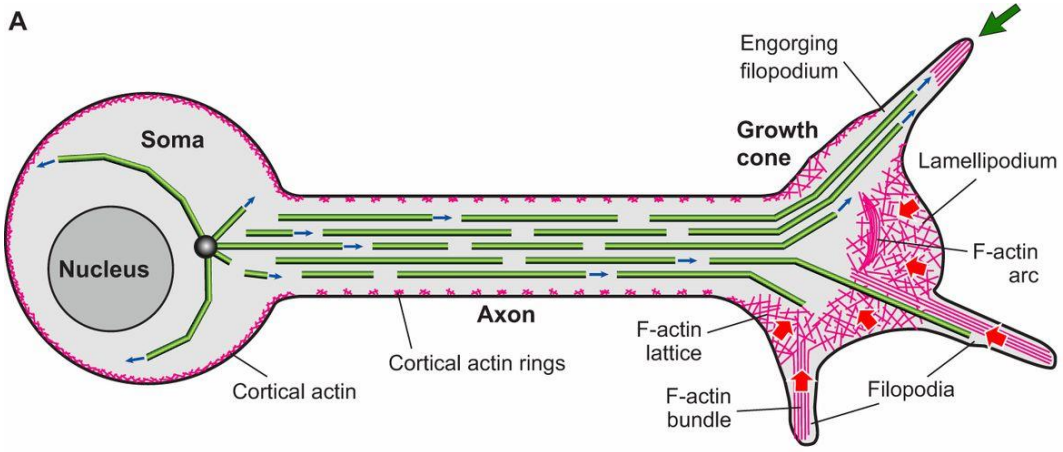

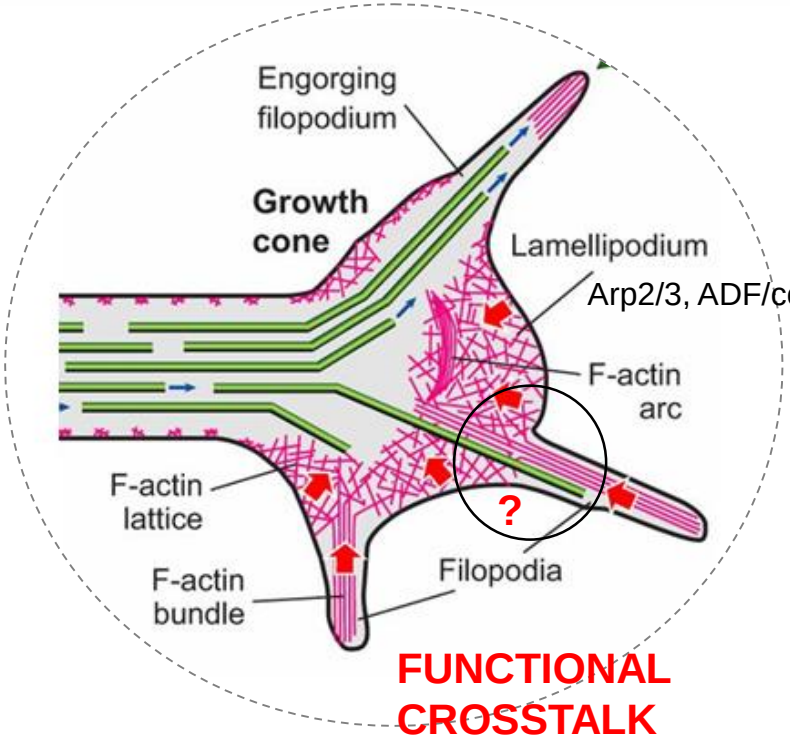

Szikora Sz., Vig A., Bugyi B. et al. JCB 2017
Vig A., Tóth M., Huber T., Pintér R., Bugyi B. et al. JBC 2017
Prokop A. et al. JCS 2013, Dent E. et al. Neuron 2003

NEURONAL CYTOSKELETON - DAAM formin in axonal filopodia formation

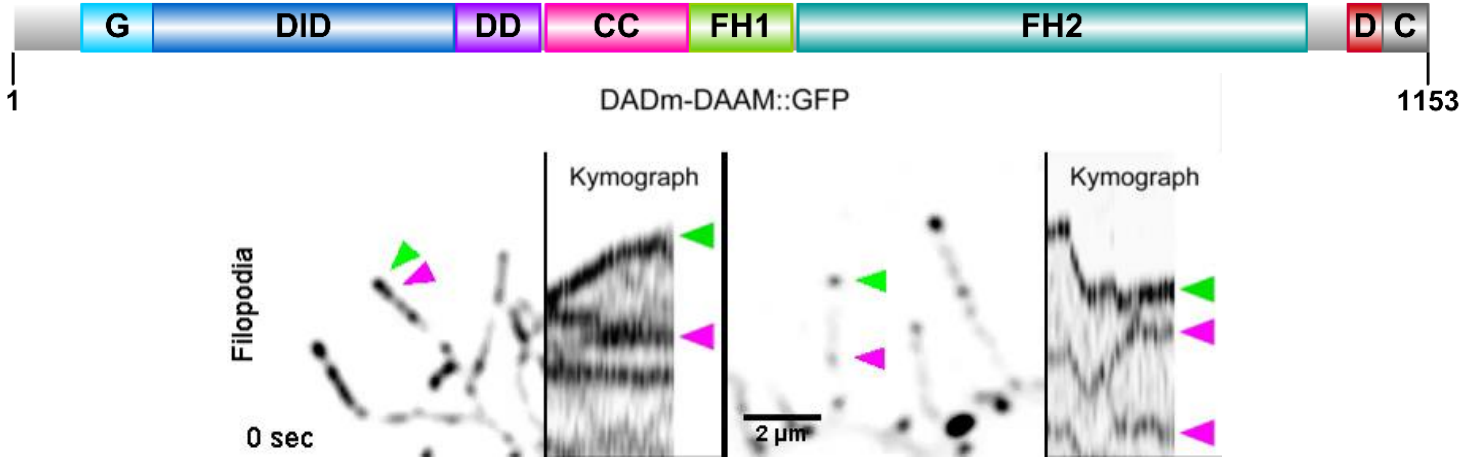

Filopodial localization and dynamics of dDAAM (in *Drosophila* primary neurons)

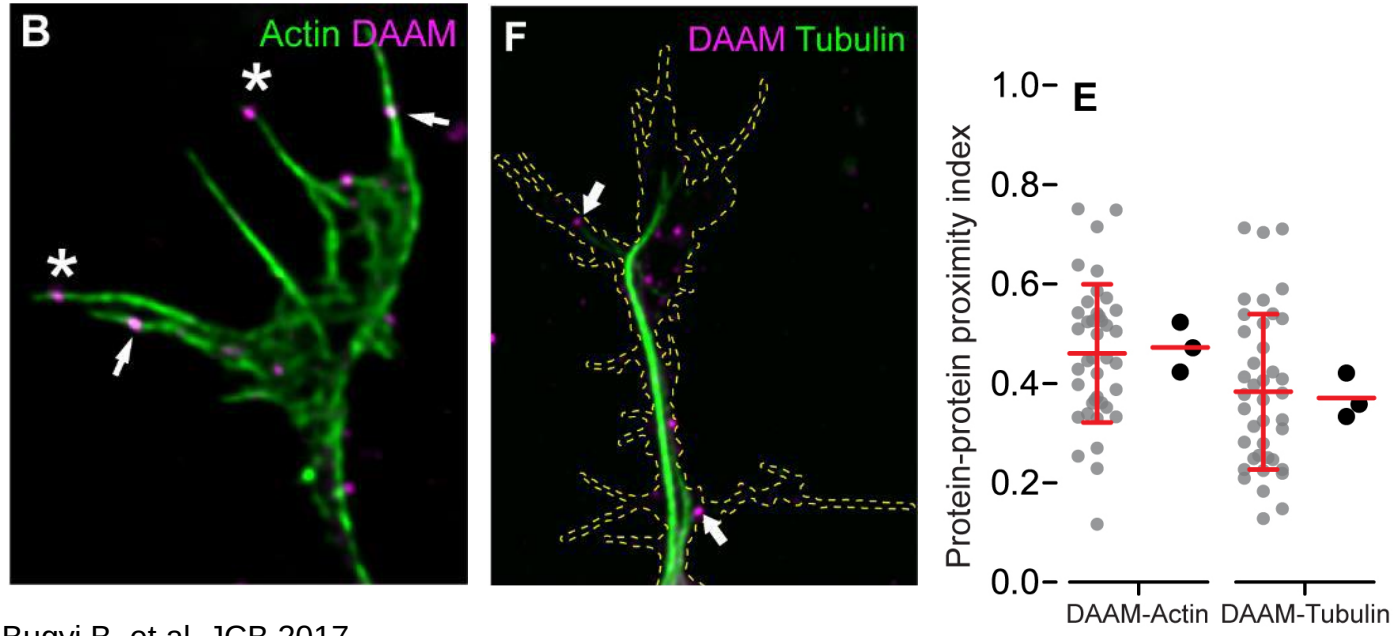

Szikora Sz., Vig A., Bugyi B. et al. JCB 2017

CONVENTIONAL FLUORESCENCE SPECTROSCOPY

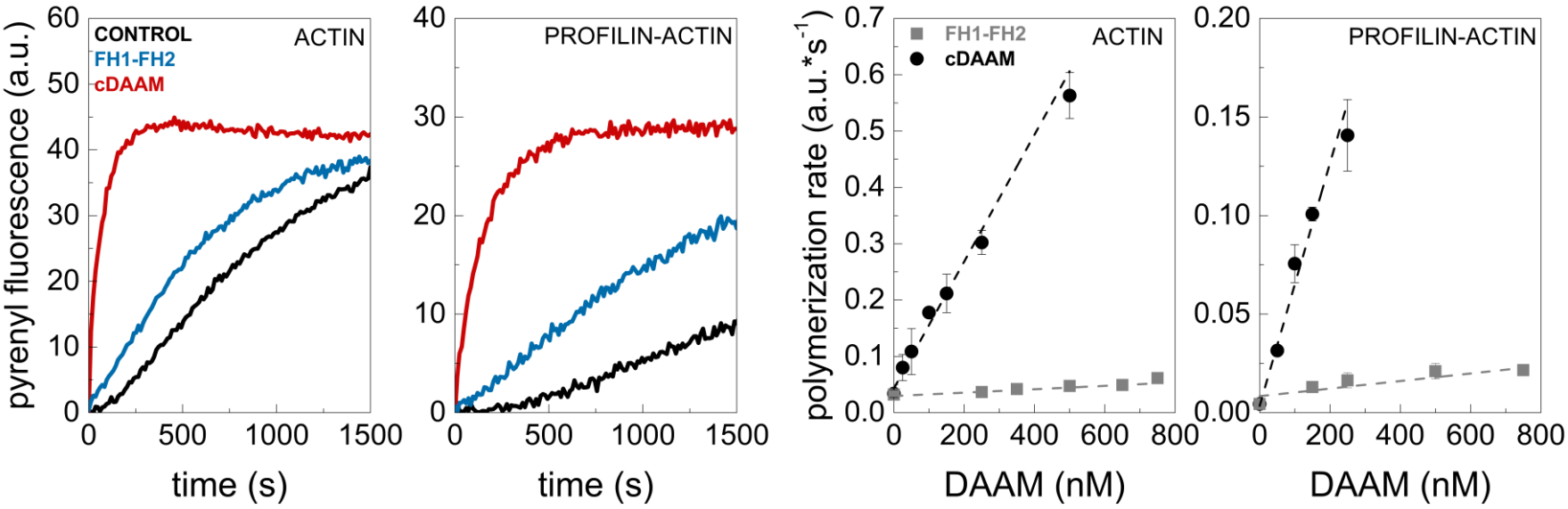

DAAM enhances actin nucleation, but inhibits filament elongation

AlexaNHS488-ACTIN (10 % LABELED)

ACTIN

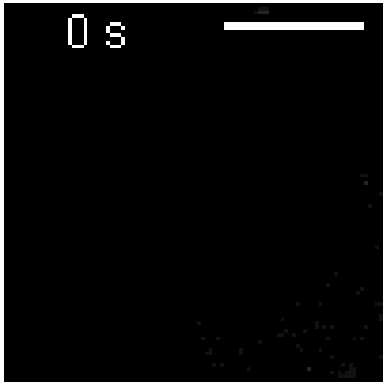

1.2 μM actin

v = 12.68 ± 0.96 su/s

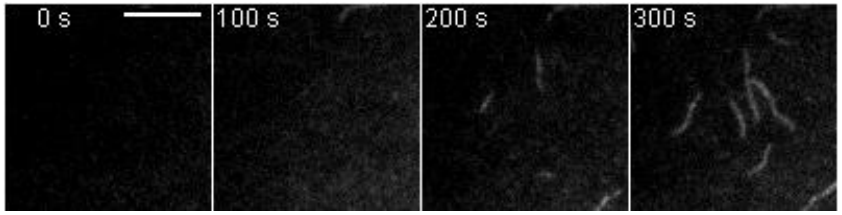

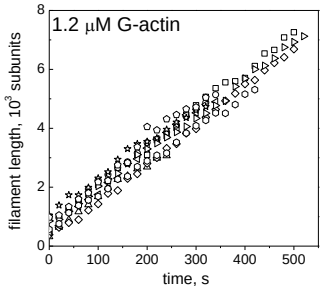

DAAM FH2

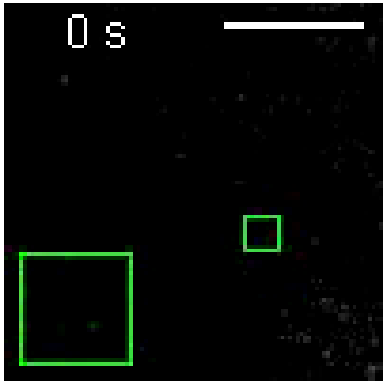

1.2 μM actin + 2.34 μM DAAM FH2

v = 0.59 ± 0.22 su/s

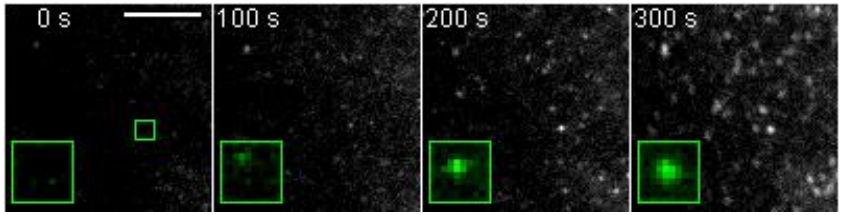

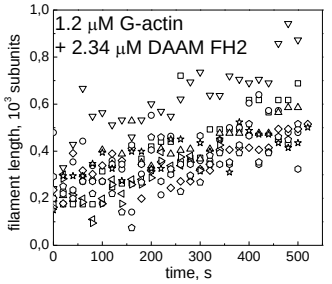

DAAM FH1-FH2

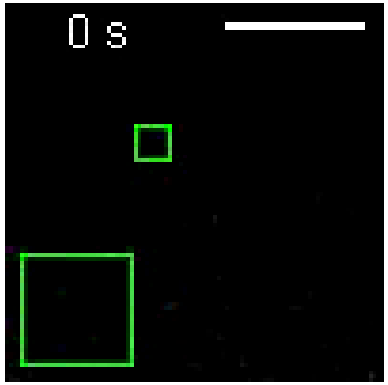

1.2 μM actin + 2.4 μM DAAM FH1-FH2

v = 0.99 ± 0.32 su/s

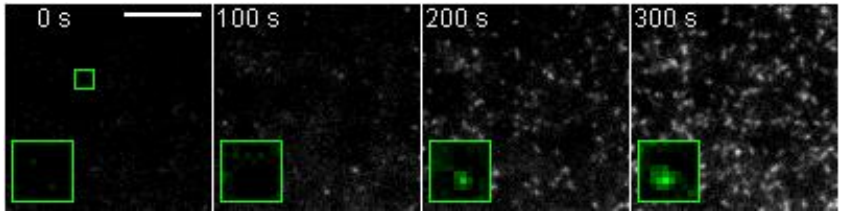

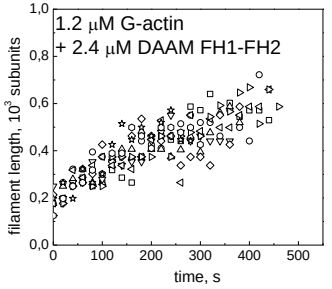

Barkó Sz. Bugyi B. et al. Journal of Biological Chemistry 2010

Profilin acts as a molecular switch in the activity of DAAM FH1-FH2

ACTIN

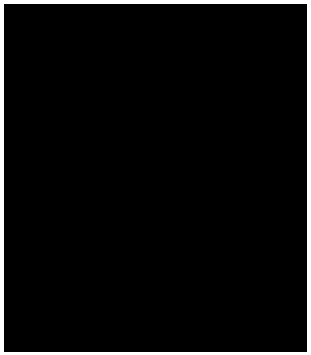

0.3 μM actin + 0.72 μM profilin

AlexaNHS488-ACTIN (10 % LABELED)
AlexaNHS568-ACTIN (10 % LABELED)

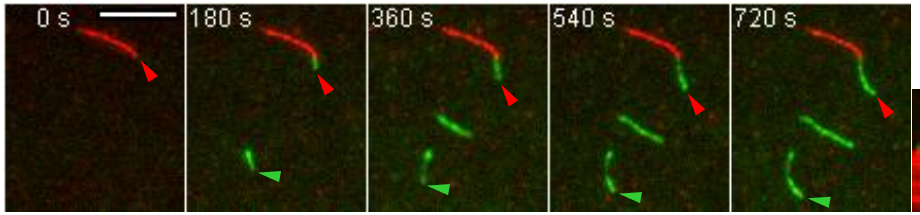

v = 2.91 ± 0.50 su/s

10 μm
500 s

DAAM FH2

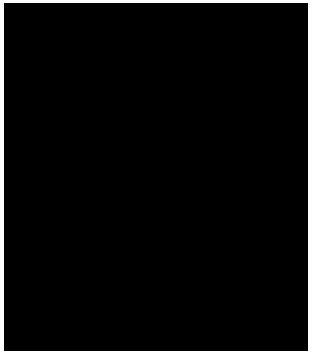

0.3 μM actin + 0.72 μM profilin + 2.6 μM DAAM FH2

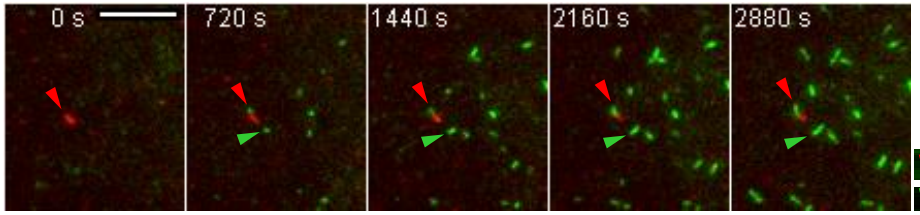

v = 0.20 ± 0.05 su/s

DAAM FH1-FH2

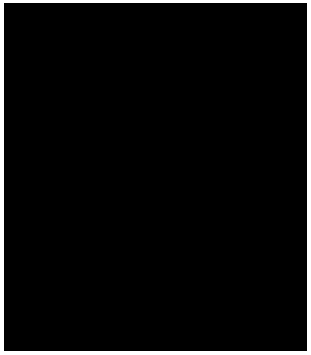

0.3 μM actin + 0.72 μM profilin + 2.4 μM DAAM FH1-FH2

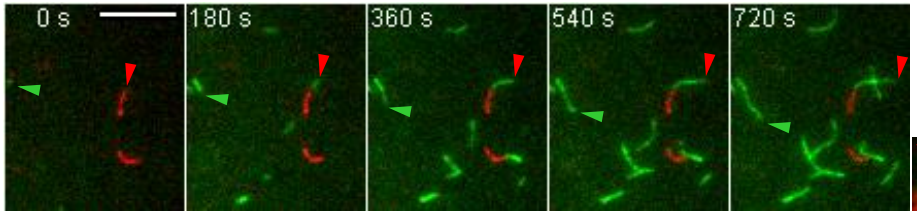

v = 2.35 ± 0.28 su/s

Barkó Sz. Bugyi B. et al. Journal of Biological Chemistry 2010

The C-terminal of DAAM further tunes the activity of the FH1-FH2 region

ACTIN

DAAM
FH1-FH2

DAAM
FH1-FH2-DAD-CT

DAAM
DAD-CT

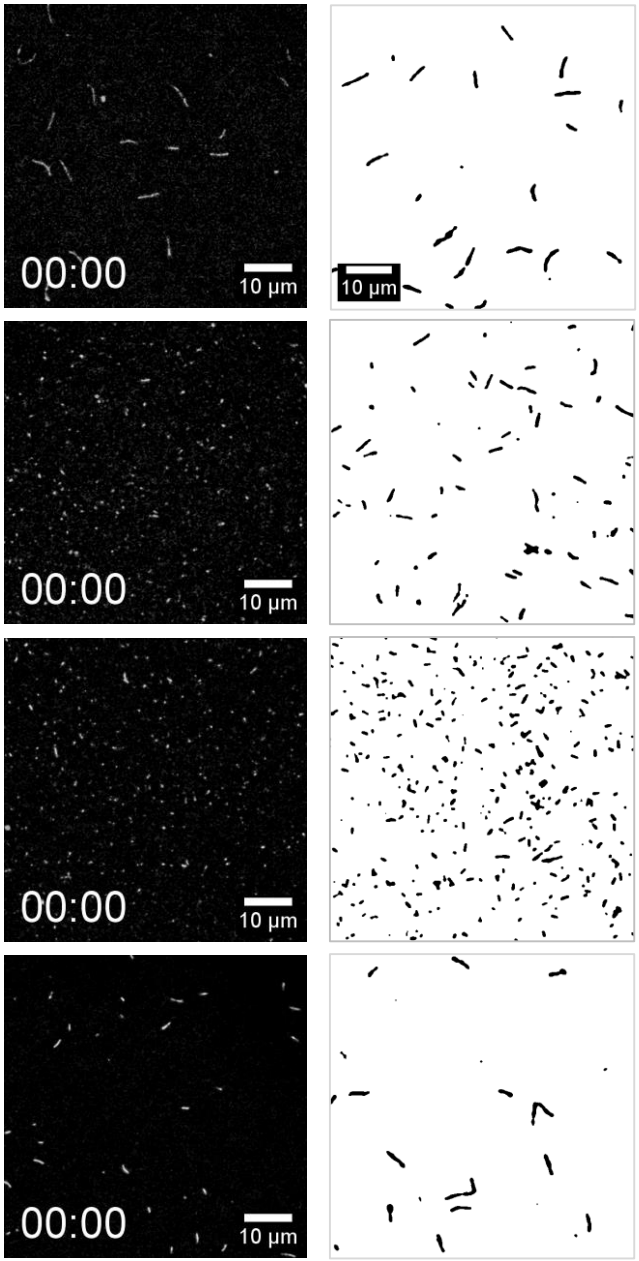

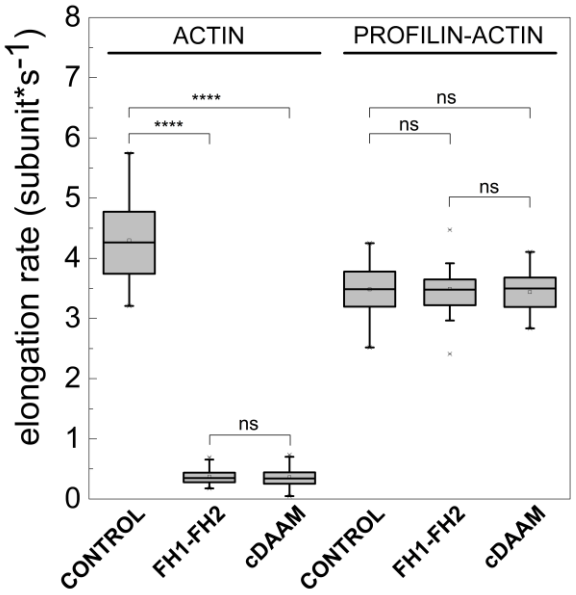

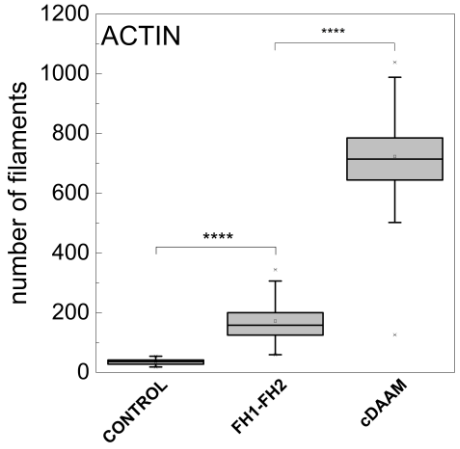

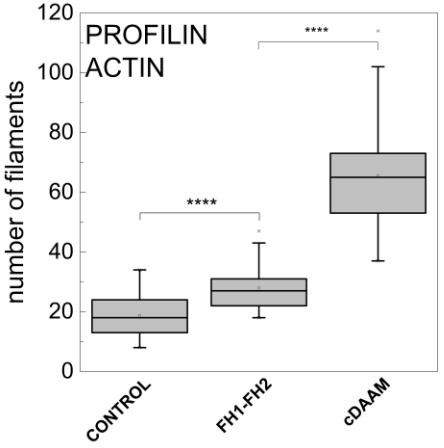

Vig A. Bugyi B. et al. manuscript in preparation 2016

The C-terminal of DAAM essential for mediating actin-microtubule crosstalk

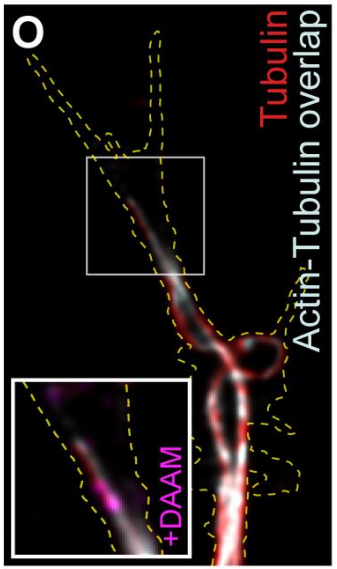

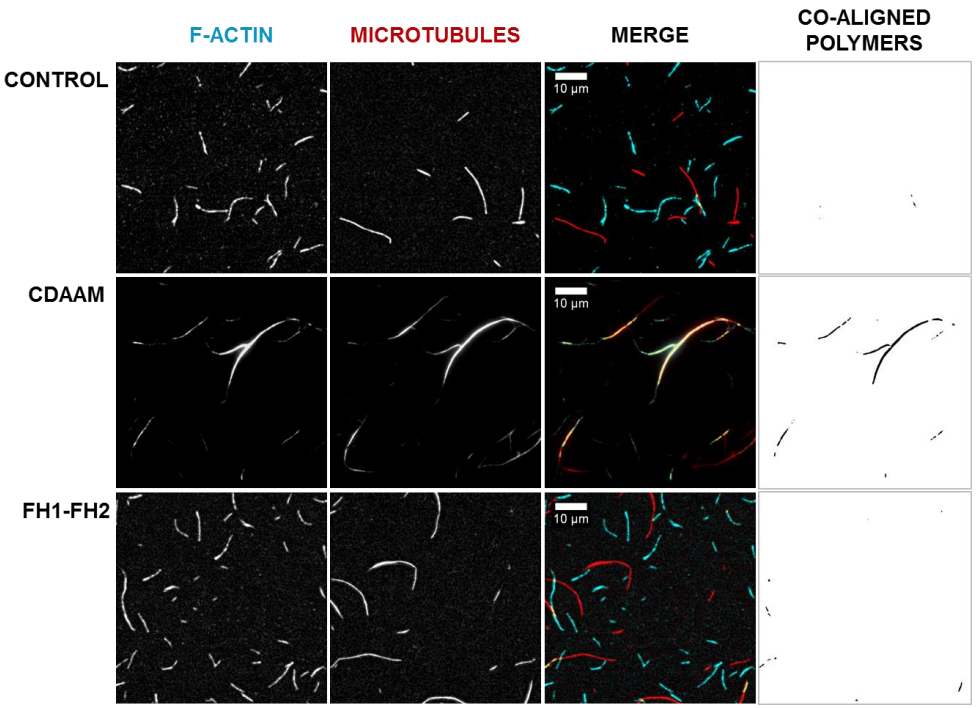

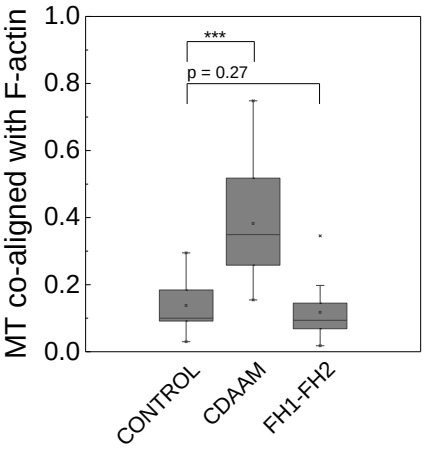

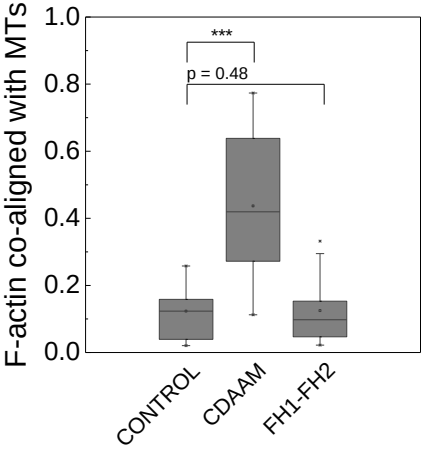

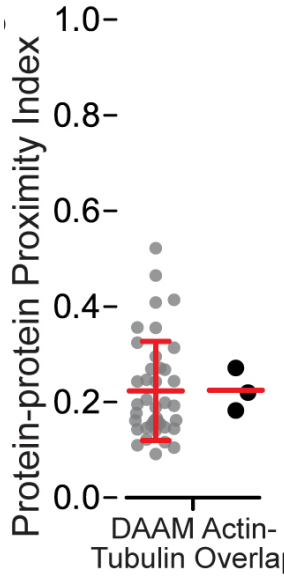

Szikora Sz., Vig A., Bugyi B. et al. JCB 2017

SCHEMATIC: DAAM MEDIATED REGULATION OF THE ACTIN-MICROTUBULE CYTOSKELETON IN NEURONS

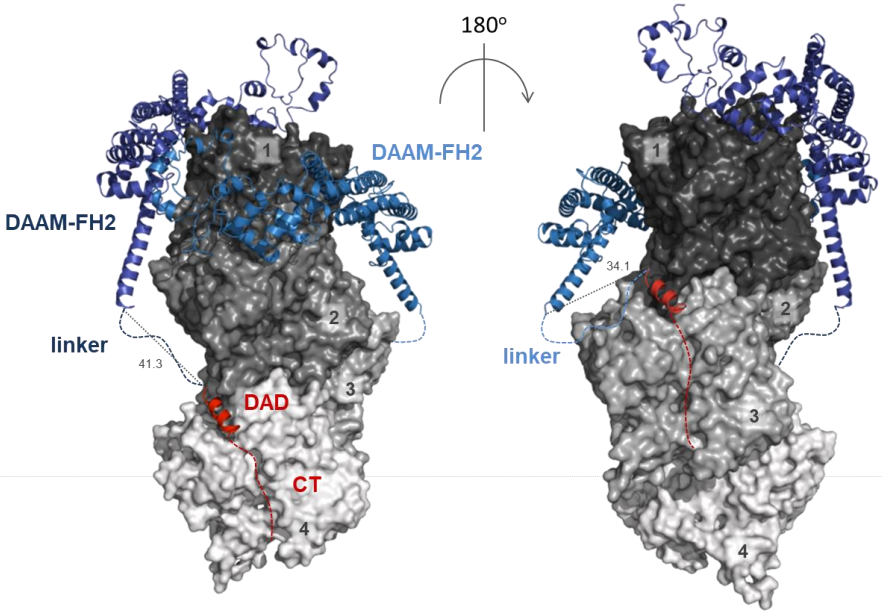

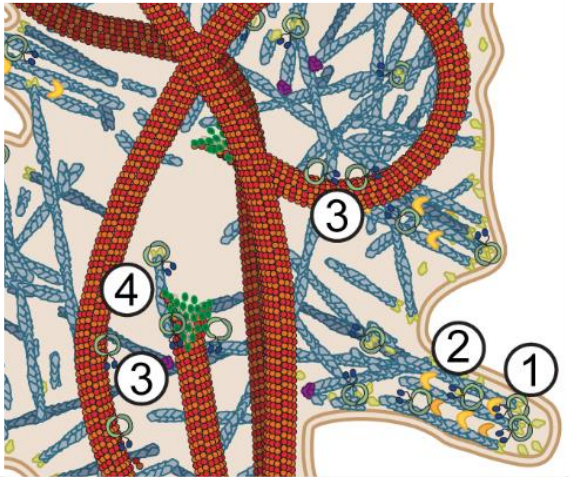

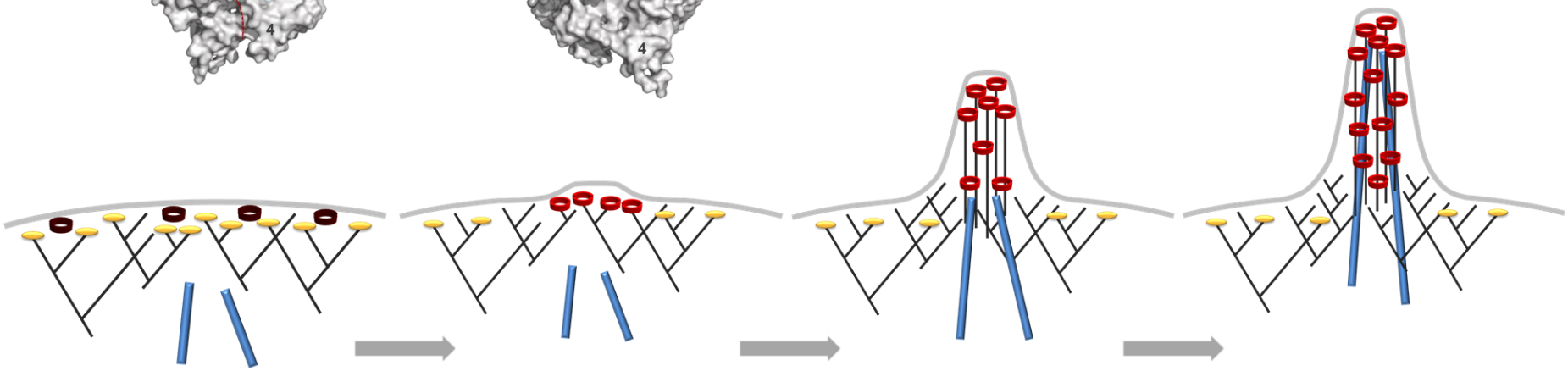

ENTANGLED ACTIN NETWORK OF LAMELLIPODIAL PROTRUSIONS
- inactive DAAM
- filament growth is terminated by CP

AT SITES OF FILOPODIAL PROTRUSIONS
- activated DAAM (RacGTPase)
- displacement of CP by DAAM

NET FILOPODIAL ELONGATION
- actin filament formation/elongation
- actin filament crosslinking

FUNCTIONAL COUPLING BETWEEN ACTIN AND MICROTUBULES
- actin filament – microtubule cross-linking

KEY MEMBRANE ACTIN MICROTUBULE CAPPING PROTEIN INACTIVE DAAM ACTIVE DAAM

Szikora Sz., Vig A., Bugyi B. et al. JCB 2017, Vig A., Bugyi B. et al. JBC 2017

TIRFM - MICROPATTERNING

Laurent Blanchoin: NRS, BIG/DRF/CEA,
Cytomorpholab Grenoble

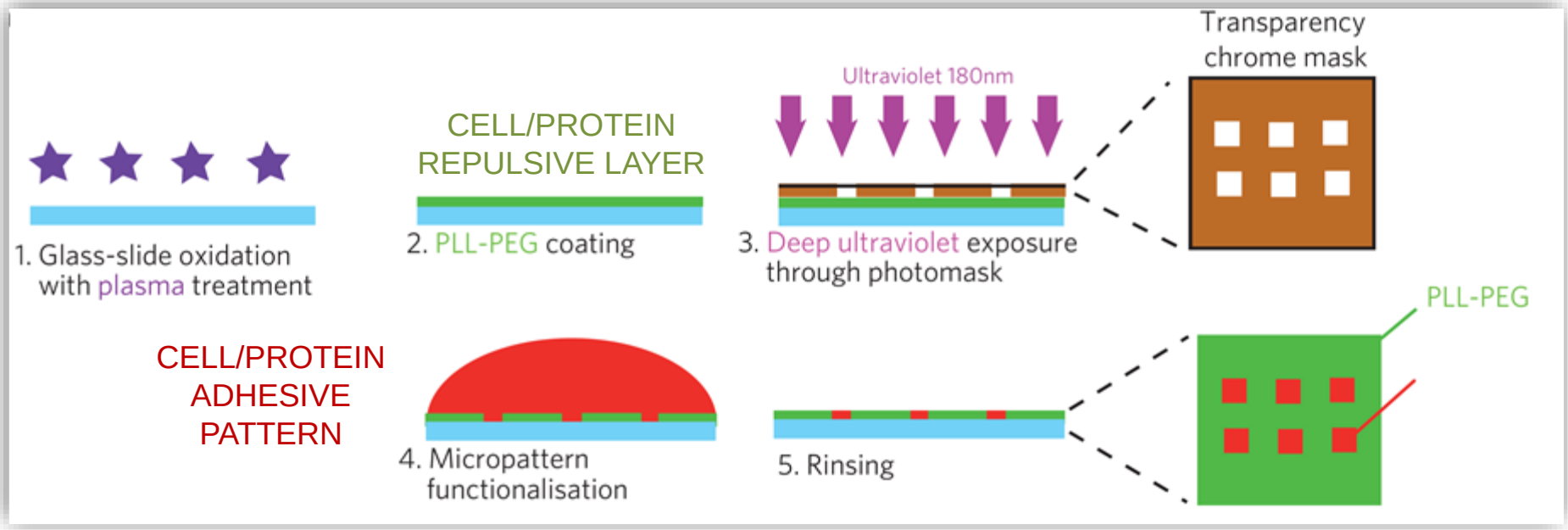

Azioune et al. Lab on a Chip 2009
Reymann AC. et al. Nature Materials 2010

Nucleation geometry governs ordered actin networks structures

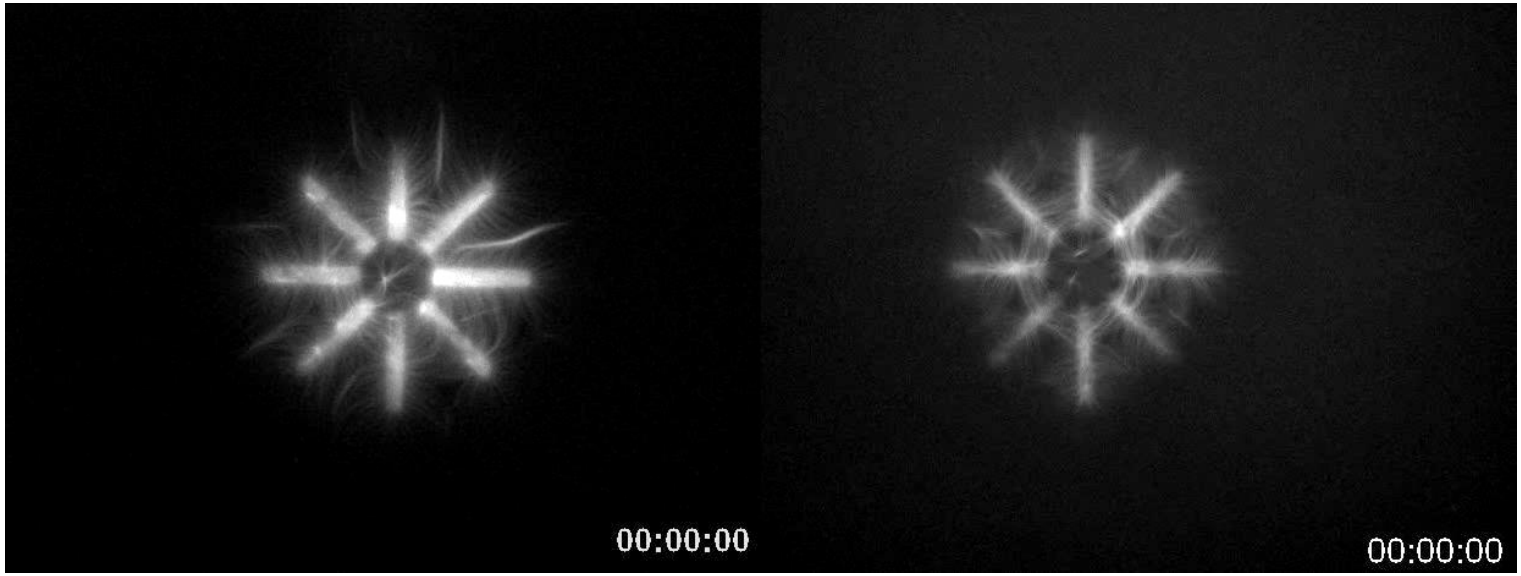

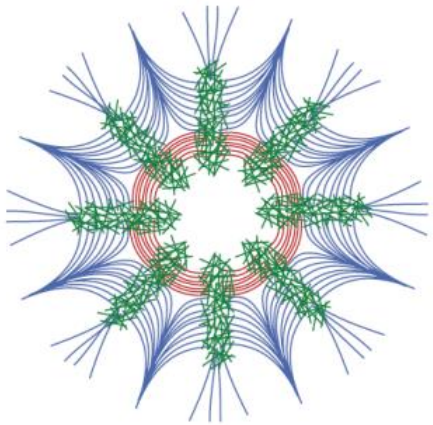

ANGLE (direction!)
BETWEEN FILAMENTS

Actin filaments :
anti-parallel
parallel
branched meshwork

PARALLEL

BRANCHED

ANTIPARALLEL

Reyman AC Science 2012
Reymann AC. et al. Nature Materials 2010

Actin network architecture can determine myosin motor activity

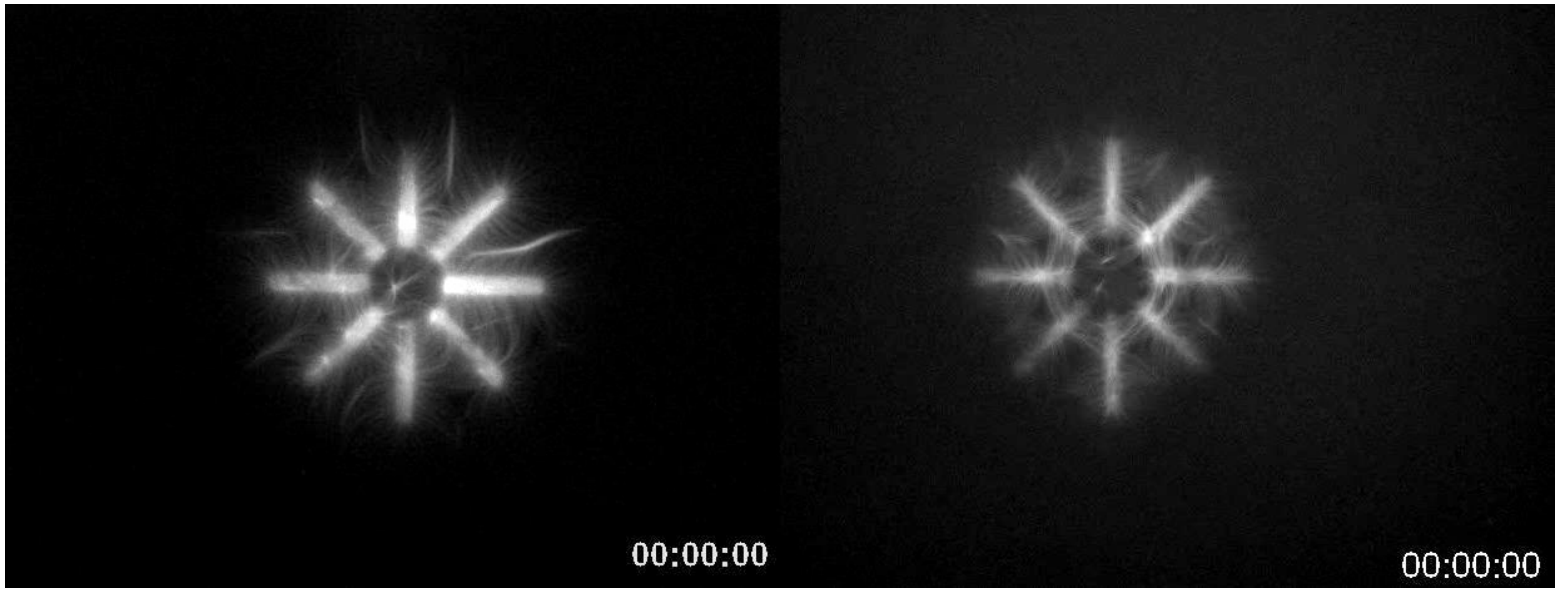

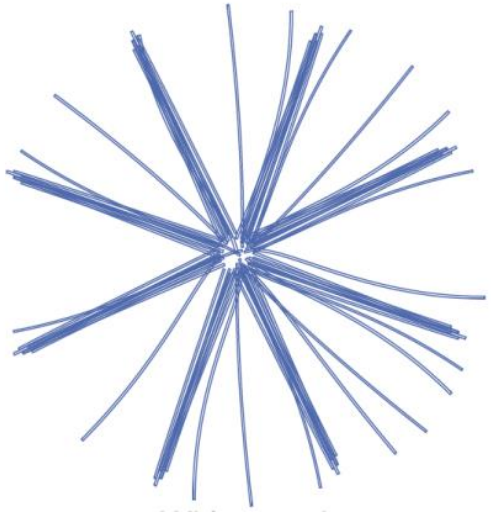

ANGLE (direction!)
BETWEEN FILAMENTS

Actin filaments :

anti-parallel

parallel

branched
meshwork

PARALLEL

BRANCHED

ANTIPARALLEL

Reyman AC Science 2012
Reymann AC. et al. Nature Materials 2010

Clathrin-mediated endocytosis: direct functional evidence for the role of actin

Uptake of receptors, membrane and cargo at the cell surface, specifically involving clathrin.

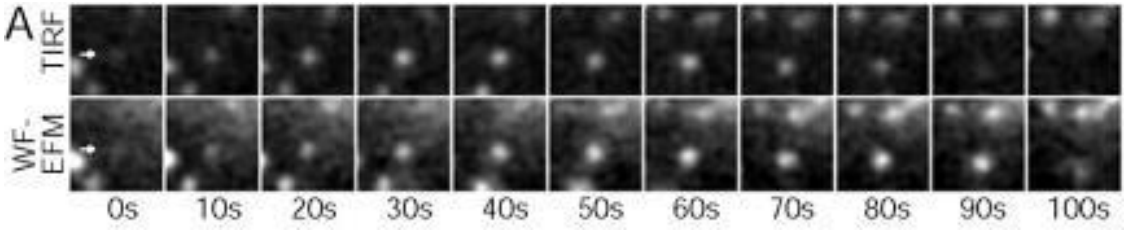

Formation and internalization of CCV.

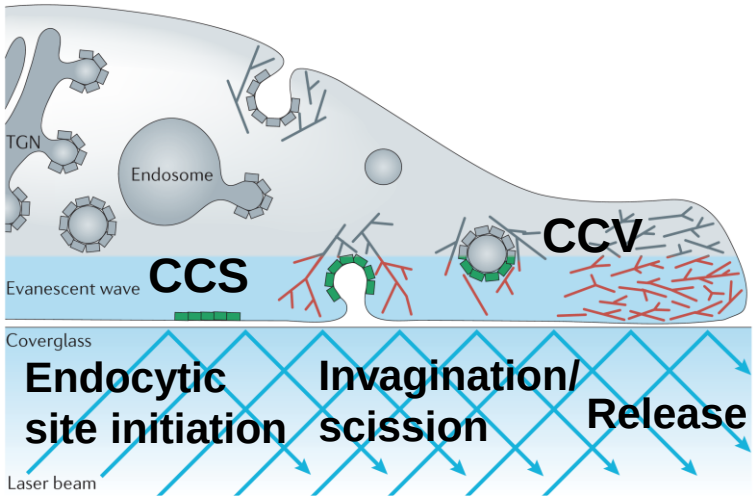

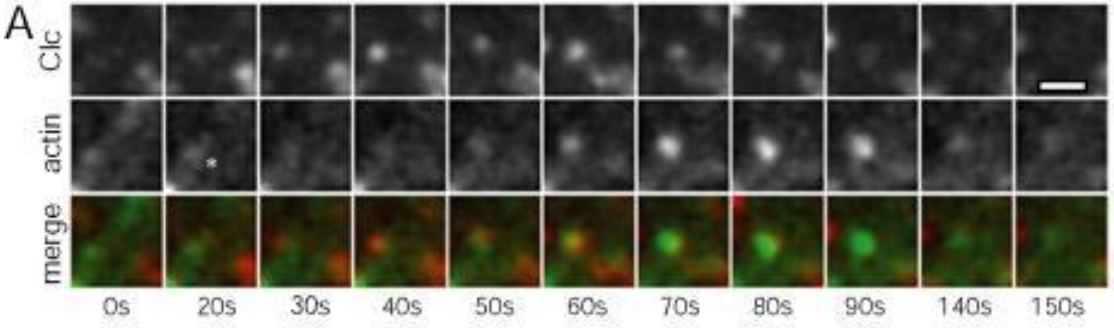

Actin and clathrin associate during endocytosis:CCS constriction, CCV internalization

Clathrin-light chain: CLC
Clathrin-coated structure (CCS): WF & TIR
Clathrin-coated vesicle (CCV) formation/internalization: selective loss of CCS from the TIRFM image

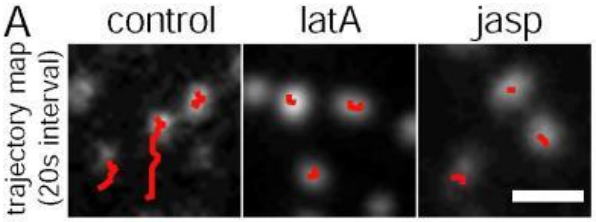

Lateral motility of CCSs requires a dynamic actin cytoskeleton.

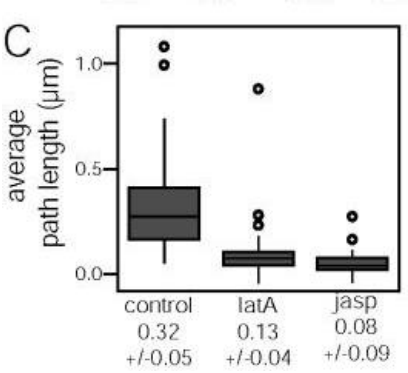

Courtesy: Kaksonen et al. Nature 2006
Yarar et al. MBC 2005, Swiss 3T3 cells

TIRFM - SINGLE MOLECULE LOCALIZATION MICROSCOPY

Image single fluorescently labelled myosin molecules to detect individual ATP turnover reactions

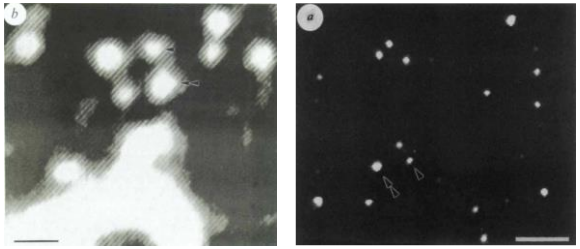

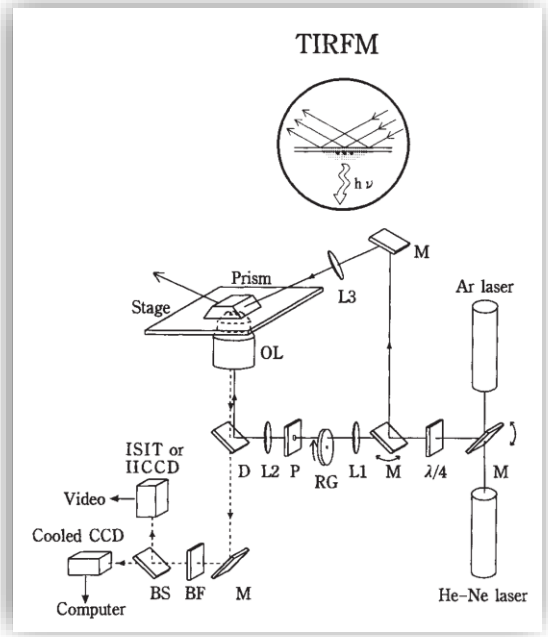

reflection fluorescence microscopy (TIRFM): the laser beam was incident on a quartz microscope slide through a 60° dispersion prism. The gap between the microscope slide and prism was filled with fluorescence-less pure glycerol. Incident angle at the quartz slide-to-solution interface was 68° to the normal (the critical angle is 66°). The beam was focused by a lens (L3) to be 100 μm × 200 μm at the specimen plane. Imaging and analysis: a cooled CCD camera (Series 4200; Astromed, UK) was used for quantitative analysis of the fluorescence intensity with low temporal resolution. For observation of rapid movement or changes in fluorescence intensity, an IICCD camera (C2400-87, Hamamatsu Photonics, Japan) or ISIT camera (C2400-08 and C2400-80H, Hamamatsu Photonics) was used.

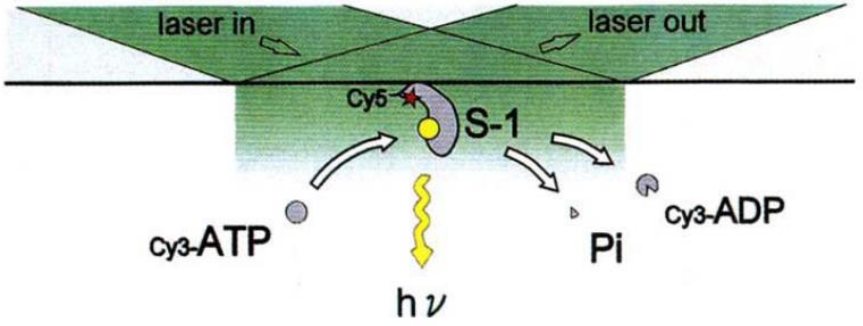

Cy5 myosin S1
670 nm, 5 mW He-Ne

Cy3 nucleotide
570 nm 3.8 mW Ar

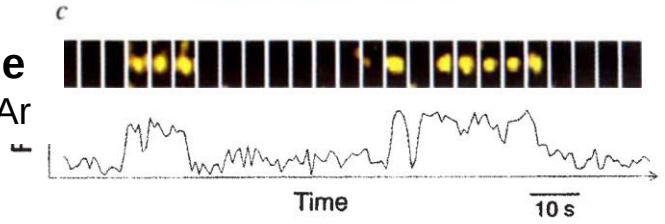

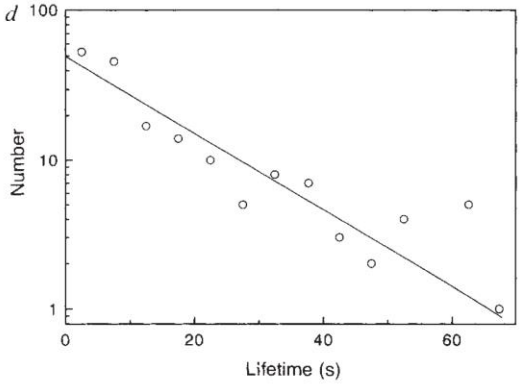

Funatsu et al. Imaging of single fluorescent molecules and individual ATP turnovers by single myosin molecules in aqueous solution. Nature 1995

Formin proteins track the growing barbed ends of actin filaments – processive actin polymerase

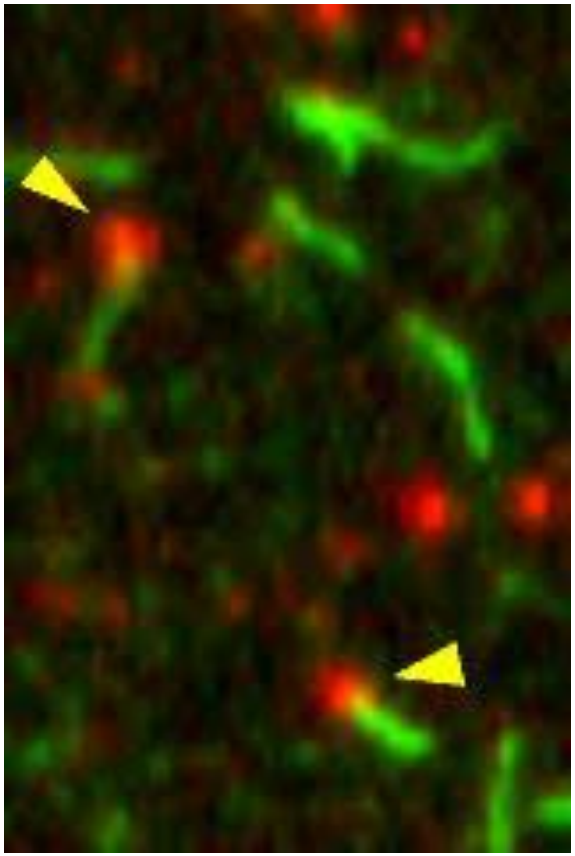

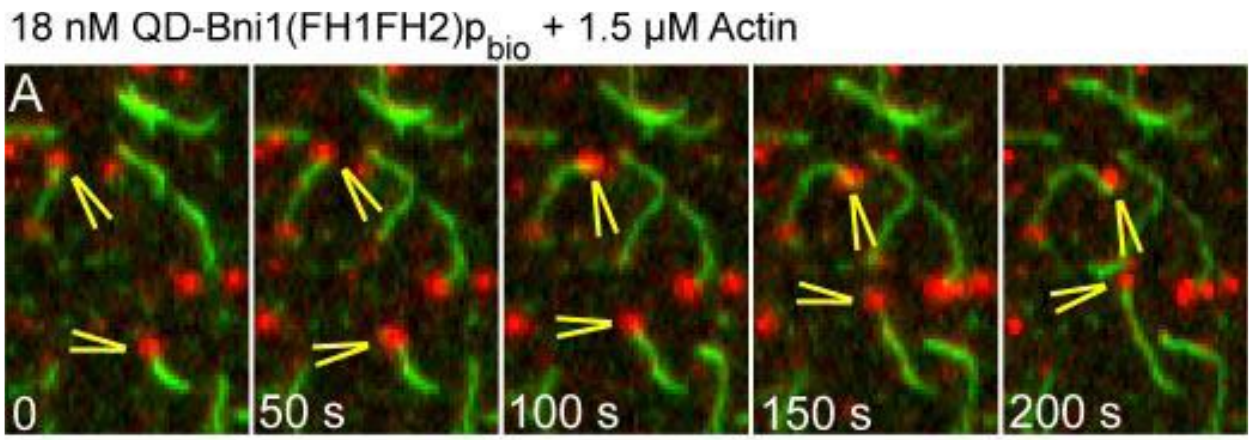

Courtesy: Paul A., Pollard T.C. JBC 2009

FORMIN: QDot 625 nanocrystal
ACTIN: Alexa488

SINGLE MOLECULE LOCALIZATION MICROSCOPY

STORM – STOCHASTIC OPTICAL RECONSTRUCTION MICROSCOPY
PALM – PHOTOACTIVATED LOCALIZATION MICROSCOPY

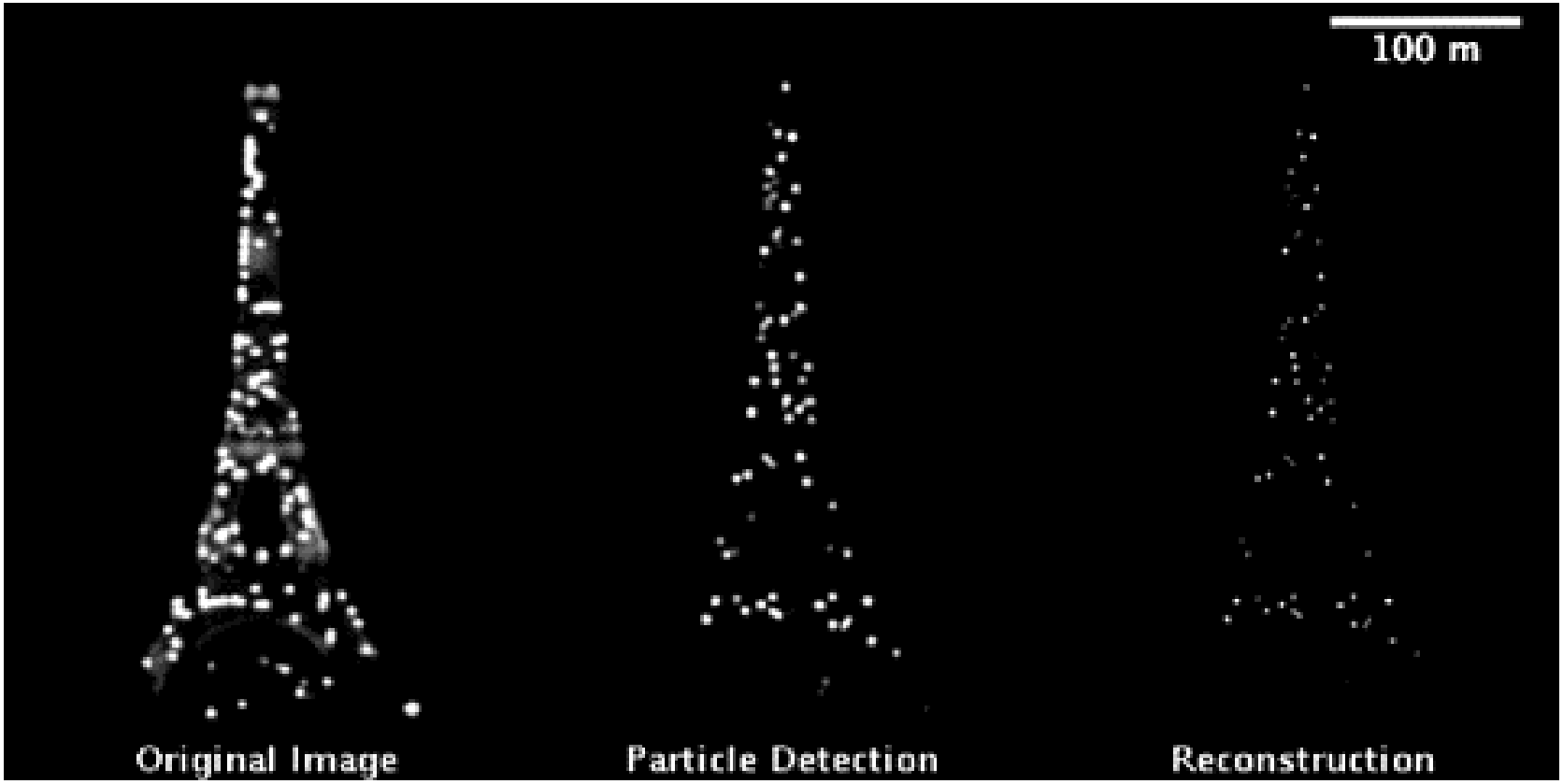

PHOTOTRANSFORMABLE FLUOROPHORES

STANDARD

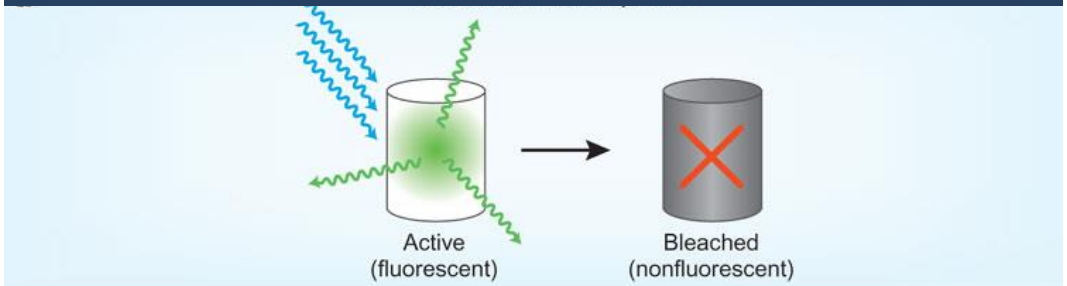

PHOTOACTIVABLE

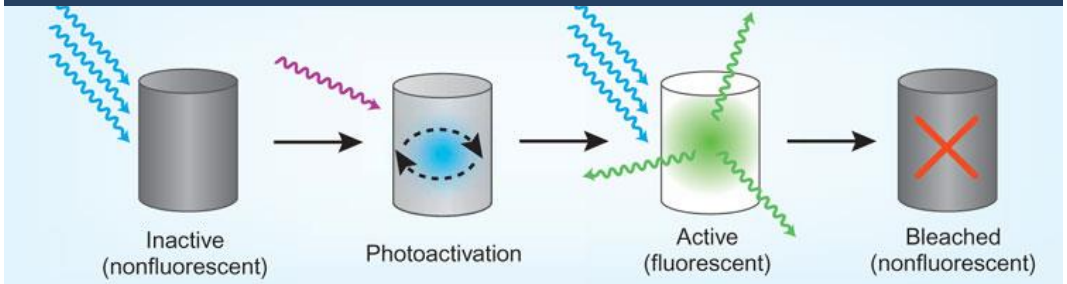

PHOTOCONVERTIBLE

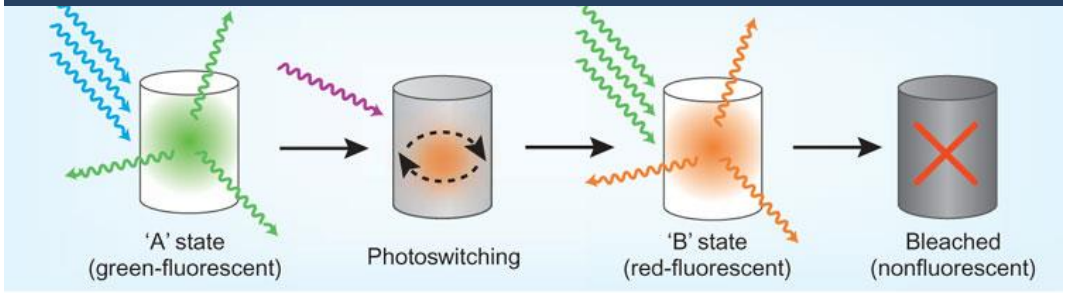

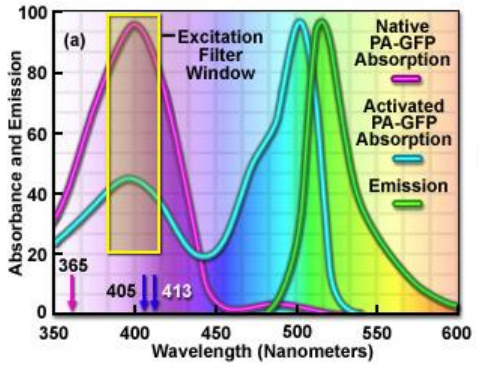

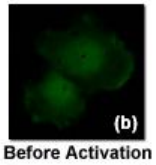

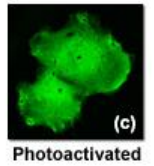

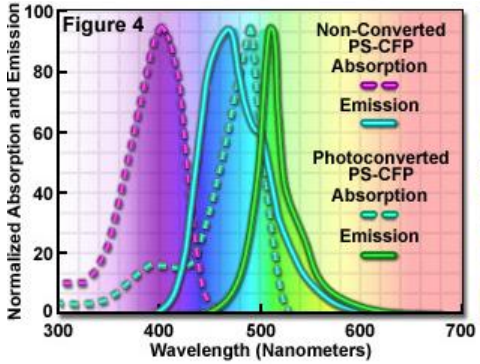

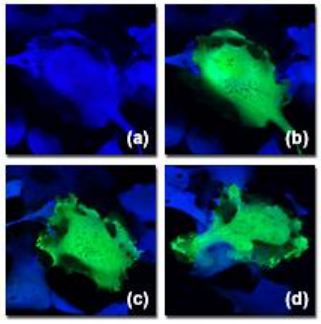

Tracking PS-CFP Labeled Cells

http://www.olympusfluoview.com/applications/opticalhighlighters.html

SINGLE MOLECULE LOCALIZATION MICROSCOPY

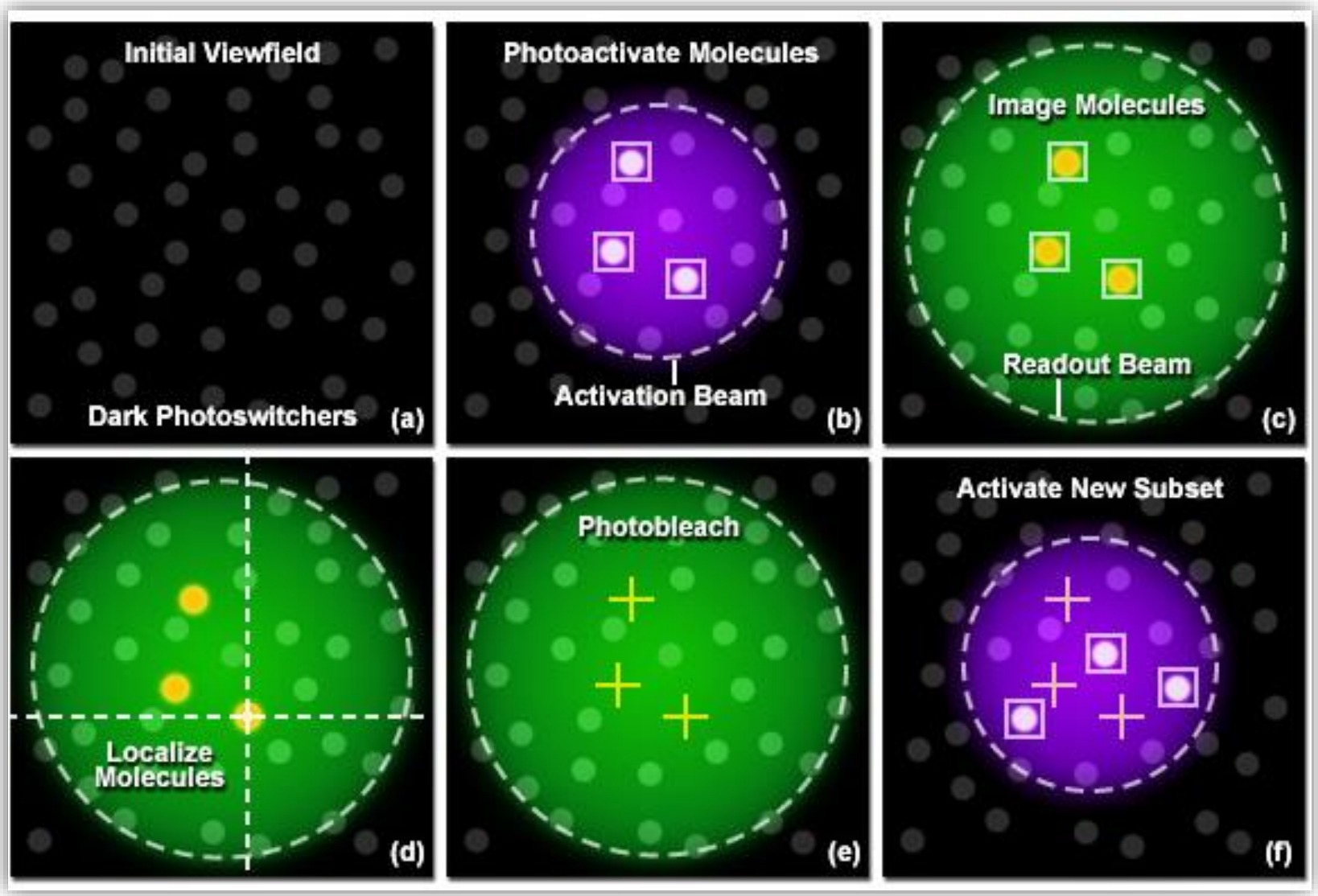

http://zeiss-campus.magnet.fsu.edu/tutorials/superresolution/palmbasics/indexflash.html

SINGLE MOLECULE LOCALIZATION MICROSCOPY

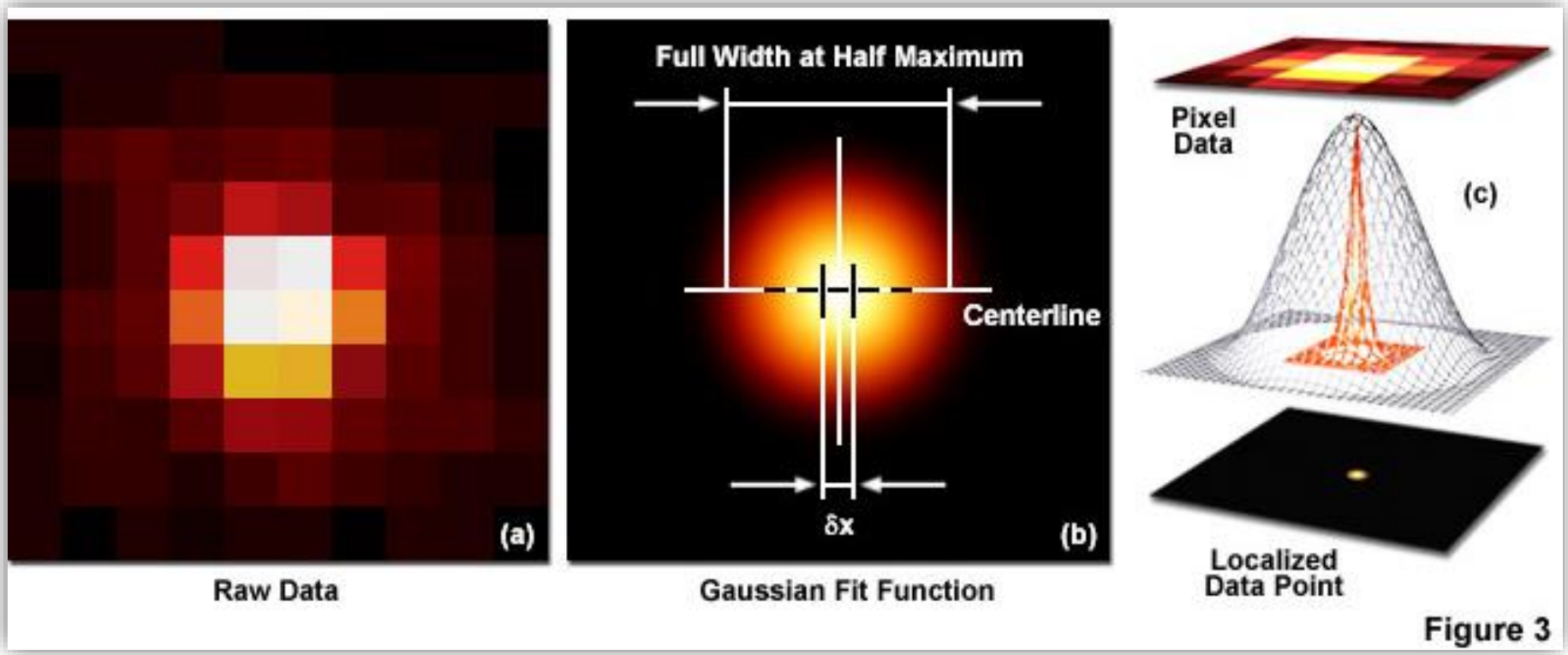

STANDARD ERROR OF PSF ESTIMATION:

$$\approx \frac{1}{\sqrt{N}}$$

SINGLE MOLECULE LOCALIZATION MICROSCOPY

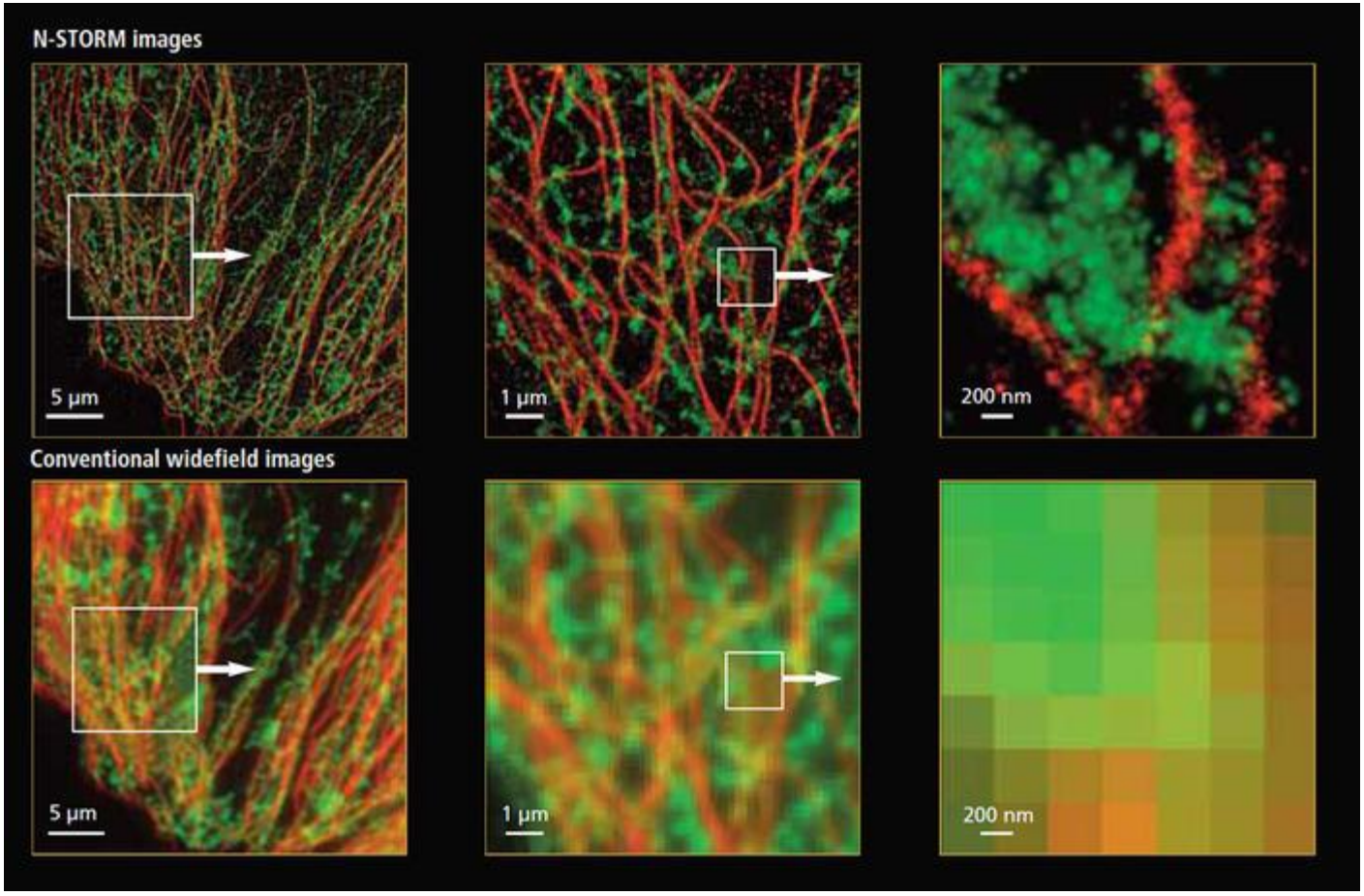

https://www.nikoninstruments.com/en_EU/Products/Super-resolution/N-STORM-Super-Resolution

SINGLE MOLECULE LOCALIZATION MICROSCOPY

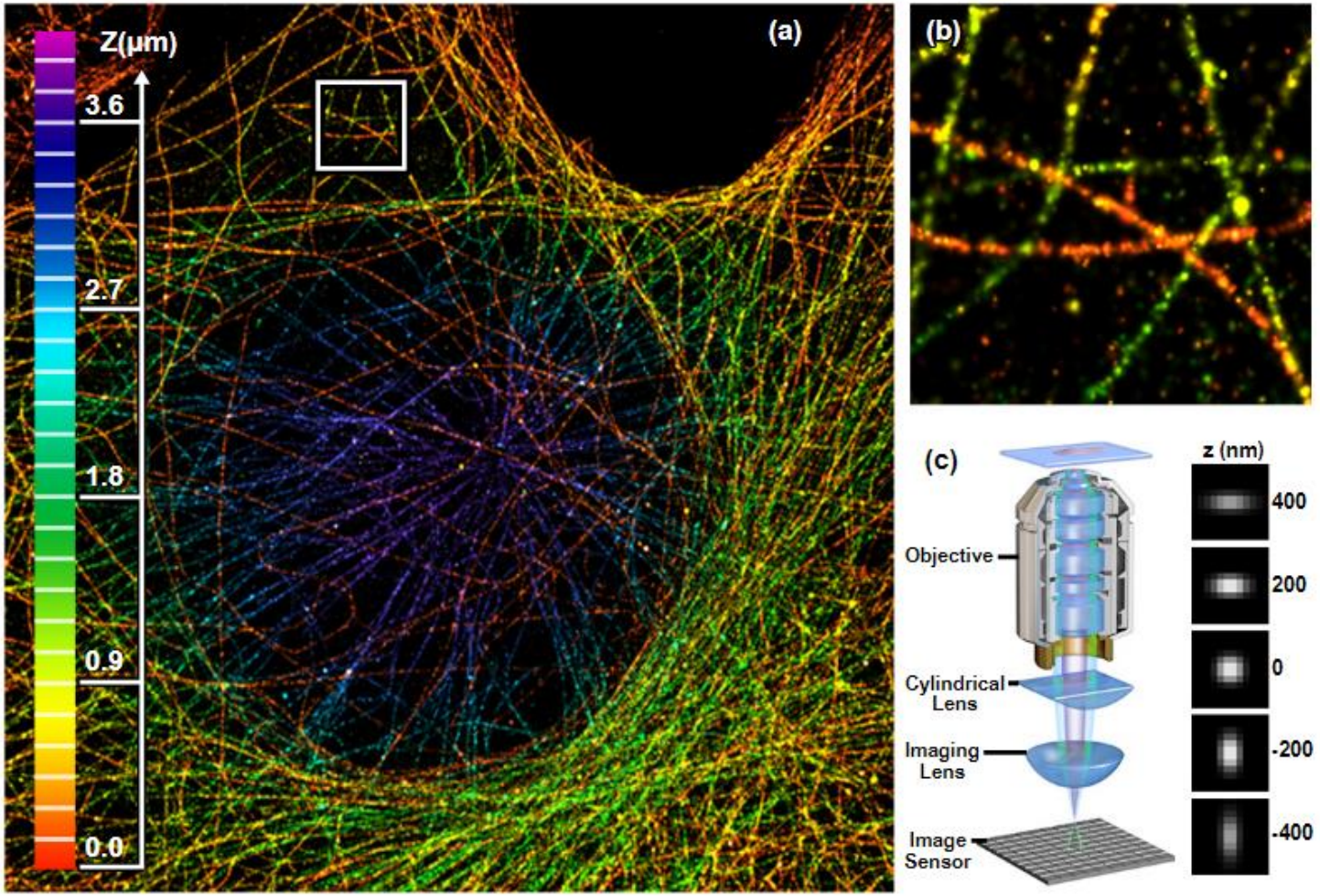

CYLINDRICAL LENS

- z-dependent shape into the PSF
- introduces astigmatism, causing the image of single emitters to be stretched in the x or y directions as a function of their z position

http://www.microscopyu.com/articles/superresolution/stormintro.html

Actin, spectrin and associated proteins form a periodic cytoskeletal structure in axons

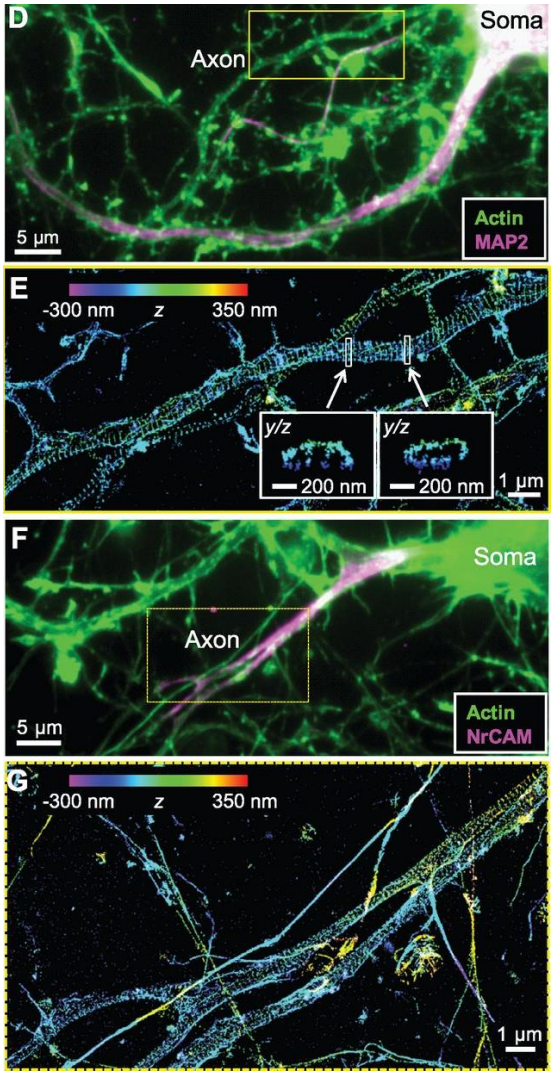

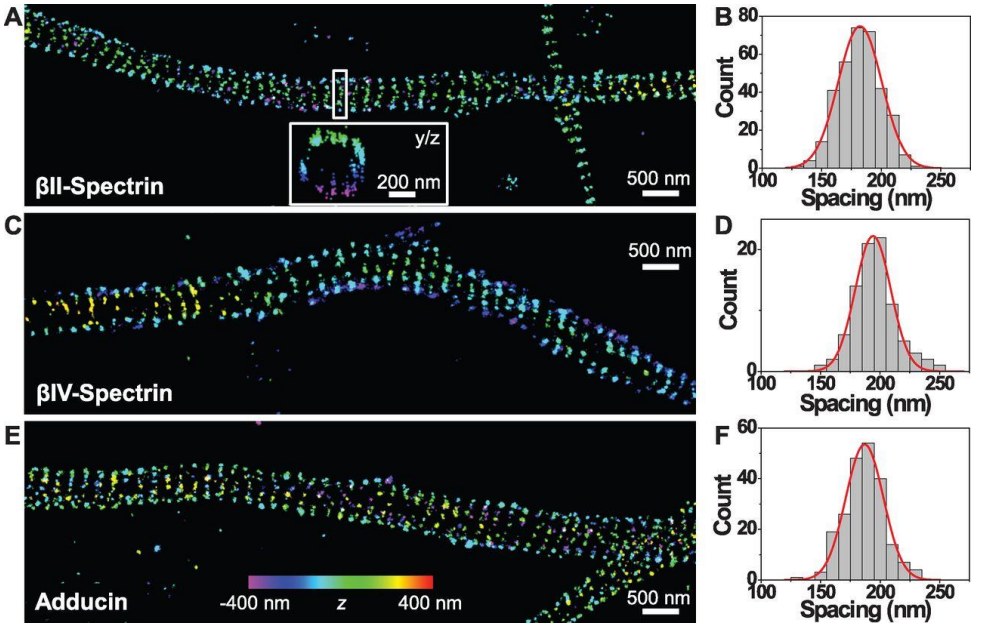

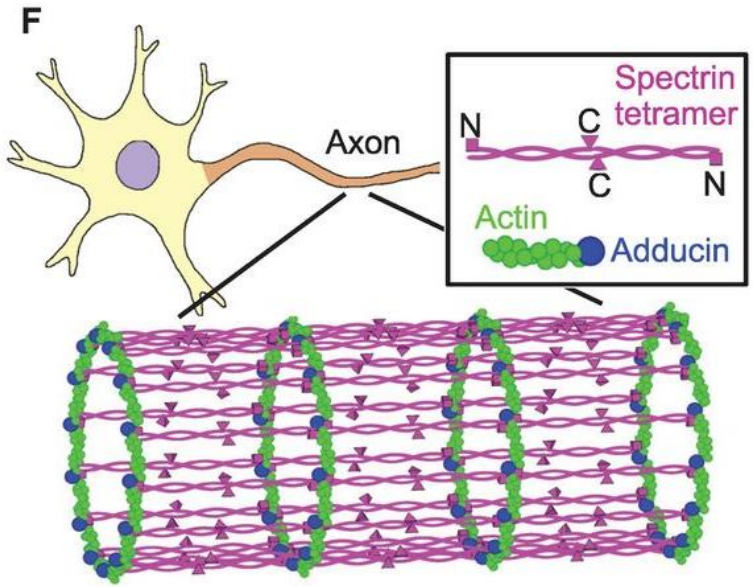

Courtesy: Zhuang et al. Science 2013

Zhuang et al. Science 2013

Periodic cytoskeletal structure in axons – revealed by SIM

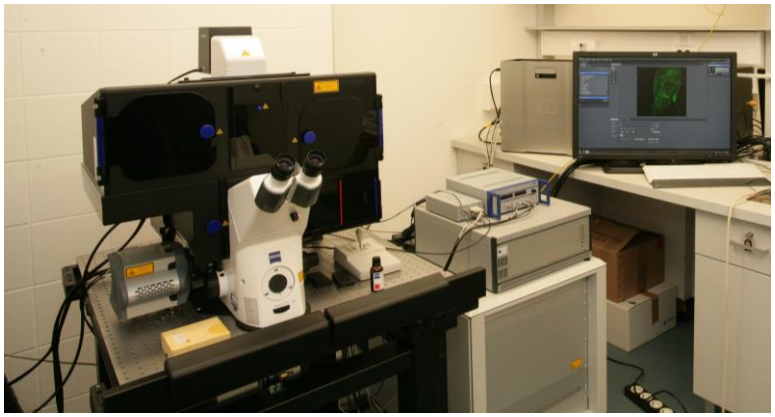

Zeiss Elyra S1 SIM
Szentágothai Research Centre, Pécs

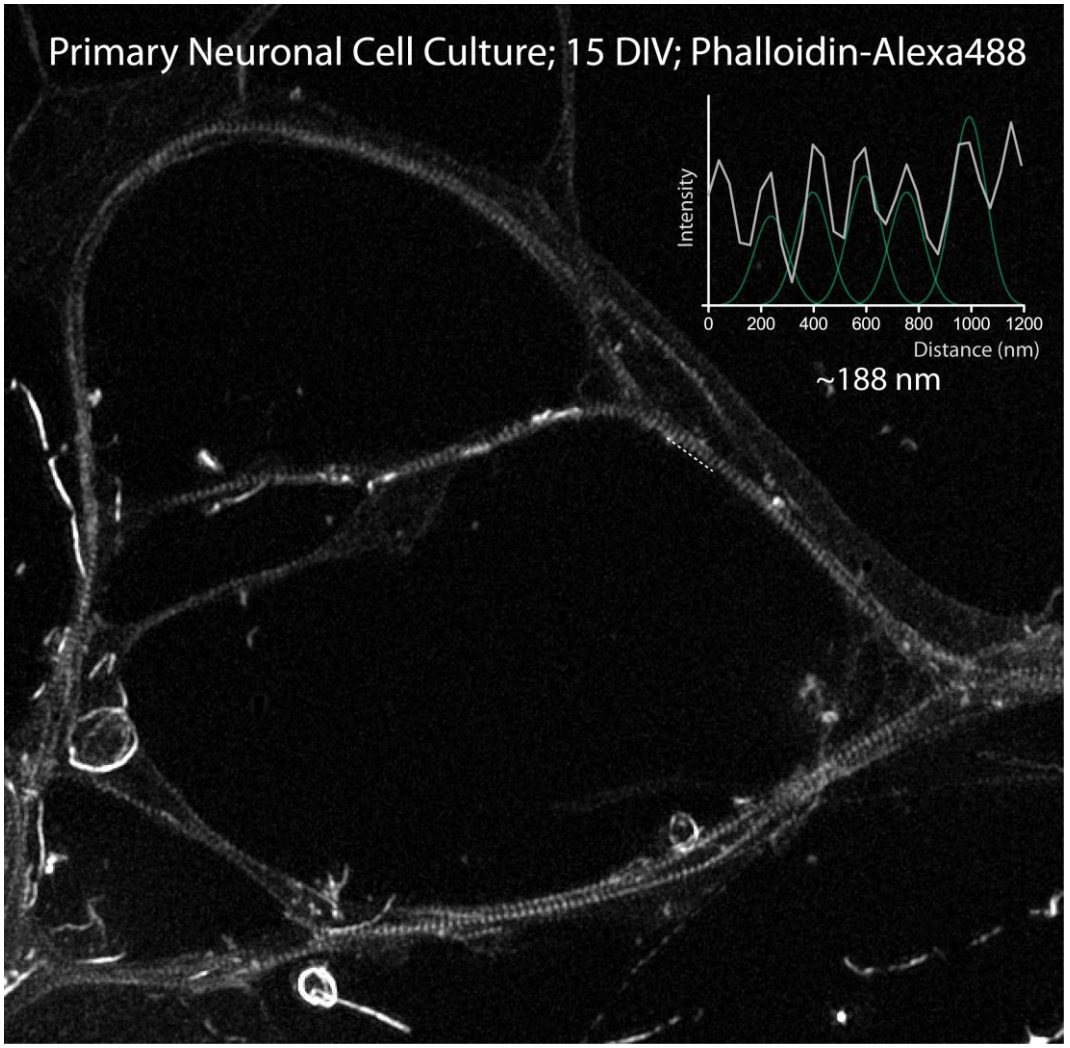

SUMMARYA

TIRFM

A NEAR-FIELD IMAGING TECHNIQUE, WHICH PROVIDES SURFACE-SELECTIVE ILLUMINATION DUE TO THE UNIQUE PROPERTIES OF THE EVANESCENT FIELD

PROVIDES RESOLUTION IMPROVEMENT (~100 nm)

USED IN CELL BIOLOGY, PROTEIN BIOCHEMISTRY STUDIES
low phototoxicity, no special fluorophores

CAN BE ADAPTED AND COMBINED WITH OTHER TECHNIQUES

CYTOSKELETAL DYNAMICS GROUP

http://cytoskeletaldynamics.wix.com/mysite

POST DOCS

Tamás Huber

PHD STUDENTS

Andrea Vig
Réka Pintér
Judit Fórizs
Mónika Tóth
Veronika Kollár

GRADUATE STUDENTS

Péter Gaszler





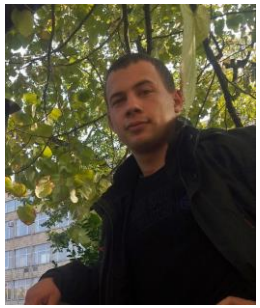

www.cnrs.fr

Marie-France Carlier
Cytoskeleton Dynamics and Motility Group
Laboratoire d'Ezymologie et Biochemie Structurales CNRS
Gif-sur-Yvette, France

József Mihály
Hungarian Academy of Sciences
Biological Research Centre
Szeged, Hungary

THANK YOU FOR YOUR ATTENTION!